Variously substituted 2-oxopyridine derivatives: extending the structure-activity relationships for allosteric modulation of the cannabinoid CB2 receptor

Francesca Gado,[⊥] Kawthar A. Mohamed,[§] Serena Meini,[⊥] Rebecca Ferrisi,[⊥] Simone Bertini,[⊥]

Maria Digiacomo,[⊥] Felicia D'Andrea,[⊥] Lesley A Stevenson,[Ψ] Robert B. Laprairie,[§]

Roger G. Pertwee,[Ψ] Clementina Manera[⊥,*]

[⊥]Department of Pharmacy, University of Pisa, 56126 Pisa, Italy. [§] College of Pharmacy and Nutrition, University of Saskatchewan, Saskatoon SK Canada. [Ψ]School of Medicine, Medical Sciences and Nutrition, Institute of Medical Sciences, University of Aberdeen, AB25 2ZD Aberdeen, Scotland, UK.

Corresponding Authors
*Clementina Manera: Phone: +39 050 2219548. Fax: +39 050 2210680.
e-mail: clementina.manera@unipi.it

ORCID
Clementina Manera: 0000-0002-7379-5743

Notes
The authors declare no competing financial interest.
RECEIVED DATE (to be automatically inserted after your manuscript is accepted if required according to the journal that you are submitting your paper to)

ABSTRACT

We previously reported the 2-oxopyridine-3-carboxamide derivative **EC21a** as the first small synthetic CB2R positive allosteric modulator which displayed antinociceptive activity *in vivo* in an experimental mouse model of neuropathic pain.

Herein, we extended the structure-activity relationships of **EC21a** through structural modifications regarding the *p*-fluoro benzyl moiety at position 1 and the amide group in position 3 of the central core. The characterization *in vitro* was assessed through radioligand binding experiments and functional assays (GTPγS, cAMP, βarrestin2). Among the new compounds, the derivatives **A1** (SV-10a) and **A5** (SB-13a) characterized respectively by fluorine atom or by chlorine atom in *ortho* position of the benzylic group at position 1 and by a cycloheptane-carboxamide at position 3 of the central core, showed positive allosteric behavior on CB2R. They enhanced the efficacy of CP55,940 in [^{35}S]GTPγS assay, and modulated CP55,940-dependent βarrestin2 recruitment and cAMP inhibition. The obtained results extend our knowledge of the structural requirements for interaction with the allosteric site of CB2R.

Keywords: CB2 cannabinoid receptor; positive allosteric modulator; 2-oxopyridine-3-carboxamide; structure-activity relationships.

1. Introduction

The endocannabinoid system (ECS) is a neuromodulatory retrograde lipid signaling system, ubiquitously expressed throughout the body and responsible for the homeostatic control of different physiological processes [1, 2]. It consists of at least 2 cannabinoid receptors (CBRs, CB1R and CB2R) members of the GPCR family, their endogenous ligands (endocannabinoids, ECs) produced on-demand from membrane phospholipid precursors, and the enzymes involved in the biosynthesis, metabolism and transport of ECs [3]. The ECS continues to attract enormous attention from the scientific community for its involvement in behavioral and brain functions, and for its therapeutic potential across an array of peripheral and neuropsychiatric diseases such as neuropathic pain, neurodegenerative diseases, cancer, glaucoma, and obesity [4]. The discovery of CB1R and CB2R in the 1990s opened the way to studies focused on the synthesis of their ligands. The biological evaluation *in vivo* and *in vitro* of these ligands suggested that the direct (i.e. orthosteric) modulation of CBRs was able to prompt several beneficial effects in the brain and in the periphery but, at the same time, it was not devoid of undesirable side effects such as mood alteration (euphoria, anxiety, panic), acute psychoses, impaired cognition, motor performance, and suicidal ideation via CB1R [5]; and immune suppression upon chronic use and, in some cases, pro-inflammatory actions via CB2R [6]. It is noteworthy that, because of these important adverse effects, few CBR-targeted ligands were able to reach an advance stage of clinical trials. Target selectivity and off-target side effects have been indicated as the 2 major limiting factors for orthosteric ligands [7]. Recently, the number of reports and studies regarding allosteric modulators of both CBRs has increased enormously [8-14]. Indeed, allosteric modulation has offered a new approach in the regulation of the ECS without any of the potential undesirable side effects associated with direct CBR interaction. Allosteric modulators interact with a receptor's allosteric site(s) which are topographically different from the orthosteric one, and this binding leads to important receptor conformational changes. In the case of mixed antagonism and negative allosteric modulation or mixed agonism and positive allosteric modulation

(i.e. ago-PAM) there might be a decrease or an increase in the activity of the receptor in the absence of the orthosteric ligand, respectively [15, 16]. Conformational changes induced by pure allosteric ligands modulate the affinity and/or efficacy of orthosteric ligands, the presence of which is essential for their activity. Allosteric modulators can be PAMs (positive allosteric modulators), NAMs (negative allosteric modulators), or NAL (neutral allosteric ligands). PAMs enhance receptor signaling which may be due either to an increased affinity, potency and/or efficacy of orthosteric ligands, or to a less efficient dissociation of orthosteric ligands [17, 18]. Moreover, PAMs can also operate by blocking receptor desensitization [19, 9]. NAMs weaken receptor responsiveness through a decrease in agonist affinity or efficacy, while NALs bind to the allosteric sites without affecting the response of the orthosteric agonist [15]. Finally, allosteric modulators can also be a combination of PAM and NAM depending on the signaling output being measured [18]. Allosteric modulators, compared to orthosteric ligands, offer several advantages which can be summarized in 4 main features responsible for their higher potential effectiveness: high specificity, target selectivity, saturability, and probe dependence [20, 21]. Indeed, allosteric site residues tend to be less conserved among receptor subtypes and can offer subtype specific targeting reducing off-target side effects [20, 22]. The tissue-specific action of allosteric ligands is due to their characteristic of exerting their effects only in tissues where ECs (or other orthosteric ligands) are present and not to compete with ligands bound to orthosteric sites. This might be useful during pathological states, in which the levels of ECs can vary significantly ‘on demand’ (e.g. they are usually higher for an autoprotective response) [23, 24]. Consequently, their effect will depend on the ECS’s tone at that time and in that tissue allowing a ‘fine tuning’ of the response with reduced probability of side effects [25]. Regarding the saturability of their effect, it is important to note that since they depend on endogenous ligands for signaling, a high concentration of allosteric modulators beyond saturation of the allosteric binding site does not have any effect in the magnitude of the allosteric effect, avoiding the risk of pharmacodynamic overdose (ceiling effect). The last point, probe dependence, refers to the fact that the same allosteric ligand may have different effects on different orthosteric ligands [26]. Moreover, allosteric ligands

may alter the signal bias of orthosteric ligands, or display ligand bias themselves. Ligand bias refers to the ability of a ligand to preferentially engage certain signaling interactions (e.g., G proteins) over others (e.g., βarrestins) [27, 28]. Since orthosteric ligands display bias *per se*, biased signaling cannot be considered a distinctive characteristic and advantage of allosteric ligands, however, specific signaling profile can further change more or less markedly, when both ligands (orthostheric and allosteric) are bound to the receptor [8, 9].

We recently described the pharmacological characterization of the 2-oxopyridine-3-carboxamide derivative **EC21a** (C2 in the paper) as CB2R PAM (Figure 1) [10]. This is the first small synthetic CB2R modulator that was correctly characterized as CB2R PAM. This evidence was obtained using [^{3}H]CP55,940 and [^{35}S]GTPγS binding assays. Moreover, **EC21a** displayed antinociceptive activity *in vivo* in an experimental mouse model of neuropathic pain [10].

In the previous work [10] we reported the influence of the replacement of the methyl and the bromine atom at position 4 and 5, respectively, of the 2-oxopyridine nucleus. In this work we present a new series of analogues of the 2-oxopyridine-3-carboxamide derivative **EC21a** that were synthesized and biologically tested in order to better understand the structural requirements for the binding to CB2R allosteric site. In particular, the structural modifications of **EC21a** involve the *p*-fluoro benzyl moiety at position 1 (**A1-A10**, Figure 1) and the amide group at position 3 (**B1-B8**, Figure 1). Firstly, with the aim to verify the importance of a substituent on the benzyl group, the *p*-fluoro benzyl group was replaced with an unsubstituted benzyl ring (**A3**). Furthermore, in order to study the stereo-electronic effects of the substituent on the benzyl group, the fluorine atom was either shifted in another position of the phenyl ring (**A1**, **A2**) or substituted with other halogen atoms (**A4-A7**). Finally, the benzyl group was replaced with aliphatic groups (**A8-A10**) to elucidate the role of π-π interaction between the substituent at position 1 of the central core and the CB2R allosteric site. Regarding the changes of the cycloheptane-carboxamide at position 3, the amide functional group was either maintained substituting the cycloheptyl ring with other aliphatic or aromatic moiety (**B1-B4**) or completely replaced by other functional groups (**B5-B8**) with the aim to optimize the

substitution on the amide function as well as to investigate the influence of the nature of the functional group in this position and the spatial requirements for the interaction of this portion of the molecule with the CB2R allosteric site.

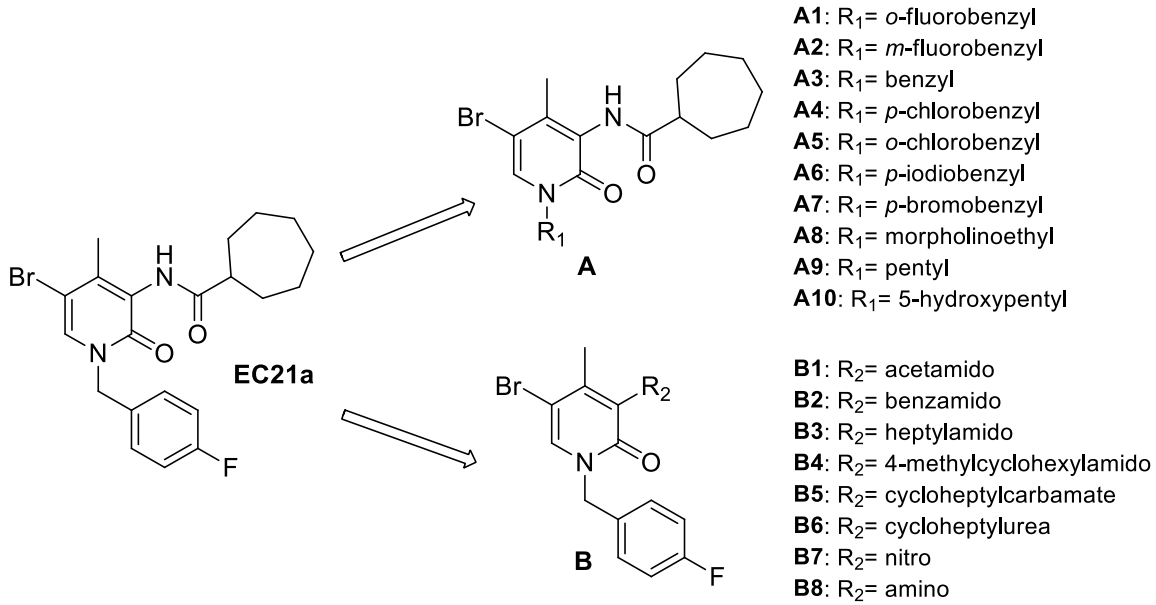

Figure 1. General structure of compound **EC21a** and of the new derivatives **A1-A10** and **B1-B8**.

Among the new compounds, **A1** (SV-10a) and **A5** (SB-13a) have been shown to be CB2R allosteric modulators. Their characterization *in vitro* was assessed through radioligand binding experiments and functional assays (cAMP, βarrestin2, GTPγS). Furthermore, the results on cAMP assay and on βarrestin2 recruitment for the parent compound **EC21a** are reported.

2. Results and discussion

2.1 Chemistry

The synthesis of compounds **A1-A8** and **B1-B6** was accomplished as depicted in Scheme 1. The commercially available starting material 2-hydroxy-4-methyl-3-nitropyridine was subjected to a *N*-alkylation reaction by treatment with NaH and LiBr in anhydrous DMF, at room temperature for 1 h and then with the appropriate benzyl chloride affording, after purification, the desired compounds **1**-

9. The *N*-alkylated derivatives **1-9** were treated with iron powder in ethanol to afford compounds **10-18**. The reaction between the amine derivatives **11-18** and the cycloheptanecarbonyl chloride in DMF and triethylamine initially at 0 °C and then at room temperature for 12 h, gave the amides **19-26** respectively. The cycloheptanecarbonyl chloride was prepared by reaction between cycloheptanecarboxylic acid and oxalyl chloride ($C_2O_2Cl_2$) at room temperature for 30 minutes. The desired 5-bromo derivatives **A1-A8** were obtained by treatment of compounds **19-26** with a solution of bromine in $CHCl_3$ at 0 °C and then at room temperature for 12 h. As reported in Scheme 1 the reaction of amine derivative **10** with the appropriate anhydride in toluene at 110°C for 16 h afforded the amide derivatives **27-29**. Compound **30** was obtained from the reaction between compound **10** and the 4-methyl-cyclohexanecarbonyl chloride, mixture of cis and trans, following the conditions above reported for compounds **19-26**. Finally, the treatment of compound **10** with cycloheptyl chloroformate (prepared from the reaction between bis(trichloromethyl) carbonate (BTC) with cycloheptanol, initially at 0 °C and then at room temperature for 2 h) in CH_2Cl_2 and triethylamine at room temperature for 4 h or with cycloheptyl isocyanate in $CHCl_3$ at room temperature for 48 h afforded the cycloheptyl carbamate derivative **31** or cycloheptyl urea derivative **32**, respectively. The desired 5-bromo derivatives **B1**-**B6** were obtained for treatment of derivatives **27-32** with bromine in the same conditions reported above.

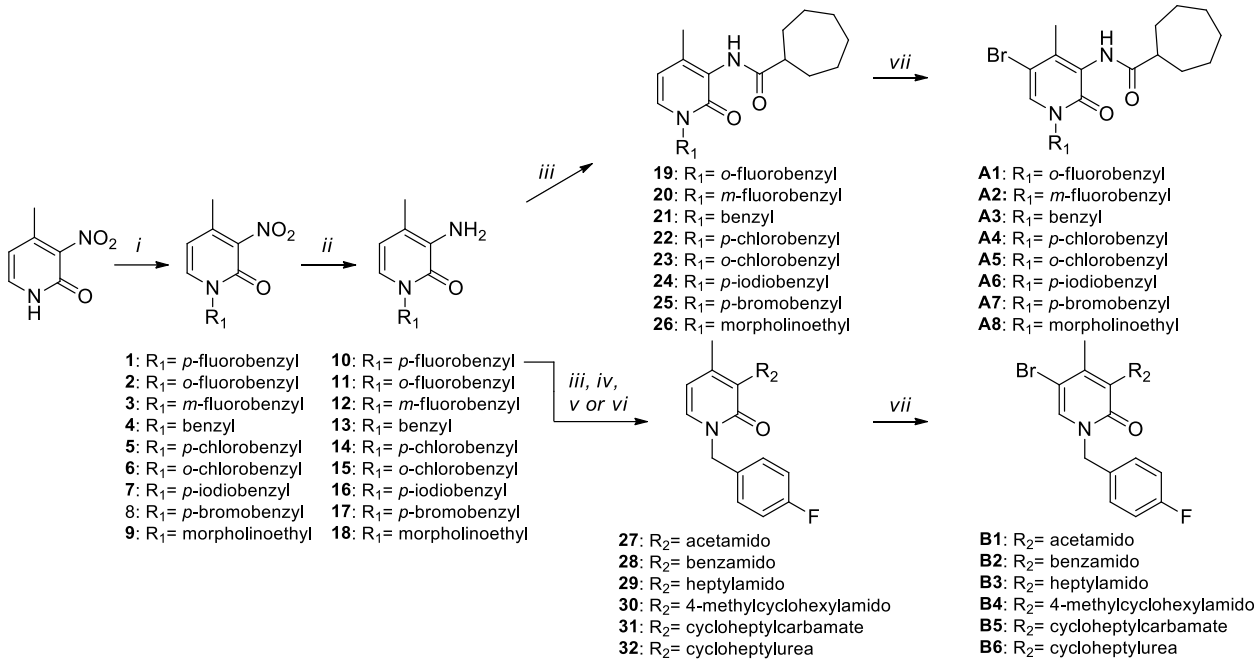

Scheme 1. Synthesis of compounds **A1**-**A8** and **B1**-**B6**. Reagents and conditions: *i*) a) NaH (60% dispersion in mineral oil), LiBr, DME, DMF, 0 °C → rt b) suitable benzyl chloride, 65 °C, 12 h; *ii*) Fe°, NH_4Cl, EtOH/H_2O (2:1), 80 °C, 3 h; *iii*) a) cycloheptanecarboxylic acid, $C_2O_2Cl_2$, rt, 0.5 h; b) DMF, Et_3N, rt, 12 h; *iv*) suitable anhydride, toluene, 110 °C, 16 h; *v*) cycloheptylchloroformate, Et_3N, dry CH_2Cl_2, 4 h; *vi*) cycloheptylisocyanate, dry $CHCl_3$, rt, 48 h; *vii*) Br_2, $CHCl_3$, 0 °C → rt, 12 h.

As reported in Scheme 2, derivatives **A9** and **A10** were synthesized starting from 2-hydroxy-4-methyl-3-nitropyridine which was treated with iron powder to obtain the amine derivative **33**. The reaction between **33** and the cycloheptanecarbonyl chloride in dry CH_2Cl_2 and NEt_3 afforded compound **34** which, by treatment with a solution of bromine in $CHCl_3$ in the same condition reported above, gave the 5-bromo derivative **35**. This compound was firstly treated with cesium fluoride in anhydrous DMF at room temperature for 1 hour, and then with the suitable halogenated reagent. The reaction mixture was stirred at 50 °C for 12 h to give the desired compounds **A9** and **A10**. For the synthesis of compound **B7**, 2-hydroxy-4-methyl-3-nitropyridine was firstly treated with bromine in $CHCl_3$ to give derivative **36**, which was *N*-alkylated following the conditions reported above. The reduction of the **B7** nitro group with iron powder in the same conditions reported above gave the desired compound **B8**.

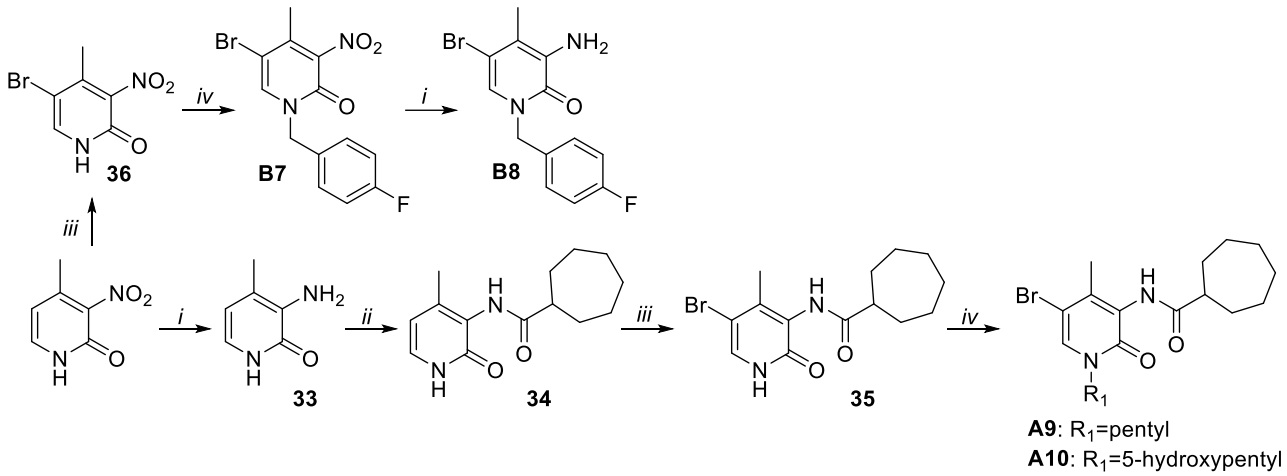

Scheme 2. Synthesis of compounds **A9, A10, B7** and **B8.** Reagents and conditions**:** *i*) Fe°, NH_4Cl, EtOH/H_2O (2:1), 80 °C, 3 h; *ii*) a) cycloheptanecarboxylic acid, $C_2O_2Cl_2$, rt, 0.5 h; b) DMF, Et_3N, rt, 12 h; *iii*) Br_2, $CHCl_3$, 0 °C → rt, 12 h; *iv*) a) CsF, dry DMF, rt; b) suitable alkyl chloride, 50 °C, 12 h.

2.2. Biological evaluation

2.2.1 [^{3}H]CP55,940 Binding Assay

Compounds **A1-A10** and **B1-B8** were evaluated for binding at hCB2R by incubating these compounds with membrane preparations obtained from Chinese hamster ovary (CHO) cells overexpressing hCB2Rs in the presence of 0.7 nM [^{3}H]CP55,940, a high-affinity orthosteric CB1R and CB2R radioligand. Initially, all compounds were screened at 100 nM. Data are displayed such that positive values indicate displacement and negative values indicate enhanced [^{3}H]CP55,940 binding (Figures 2-4). The results showed that the most of the compounds either partially displaced [^{3}H]CP55,940 or were completely inactive (Figure 2). On the contrary, compounds **A1**, **A5**, and **A7**, enhanced the binding of the radioligand to hCB2R.

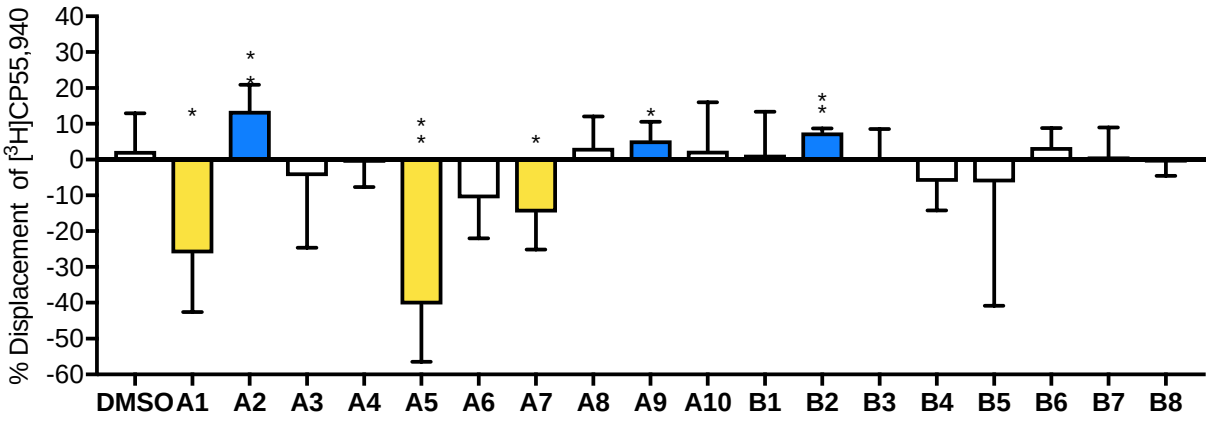

Figure 2. Preliminary screening of [^{3}H]CP55,940 displacement from hCB2R with 100 nM compounds **A1-A10** and **B1-B8**. Yellow columns indicate compounds that increase the binding of [^{3}H]CP55,940; blue columns indicate compounds that decrease the binding of [^{3}H]CP55,940; white columns indicate no significant difference. *$p < 0.05$; **$p < 0.01$ relative to 0 as determined by non-overlapping 95% confidence intervals. Data are mean with 95% confidence intervals of 3-6 independent experiments.

More specifically, compounds **A1** (SV-10a**)**, **A5** (SB-13a**)** and **A7** (SB-16a**)** were the most effective at 100 nM. Subsequent experiments tested the ability of **A1** (SV-10a**)**, **A5** (SB-13a**)** and **A7** (SB-16a**)** to increase [^{3}H]CP55,940 binding to hCB2R in a concentration-dependent (1 nM - 10 µM) manner. hCB2R binding data indicated that **A1** (SV-10a) and **A5** (**S**B-13a) induced approximately 20% and 40% increases in the binding of [^{3}H]CP55,940, respectively, between 1 nM and 1 µM (Figure 3). **A7** (SB-16a) affected the binding of [^{3}H]CP55;940 only to a negligible extent (Figure 3). Because compound concentrations below 1 nM were not tested, we do not estimate the affinity of these compounds for hCB2R here in this initial report of **A1** (SV-10a**)**, **A5** (SB-13a**)** and **A7** (SB-16a**)** pharmacology. Enhancement of hCB2R binding was lost at 10 µM (Figure 3), which may have resulted from off-target effects not assessed here and beyond the scope of the present study. Overall, these data suggest **A1** (SV-10a) and **A5** (SB-13a) may be hCB2R PAMs at concentrations below 1 µM.

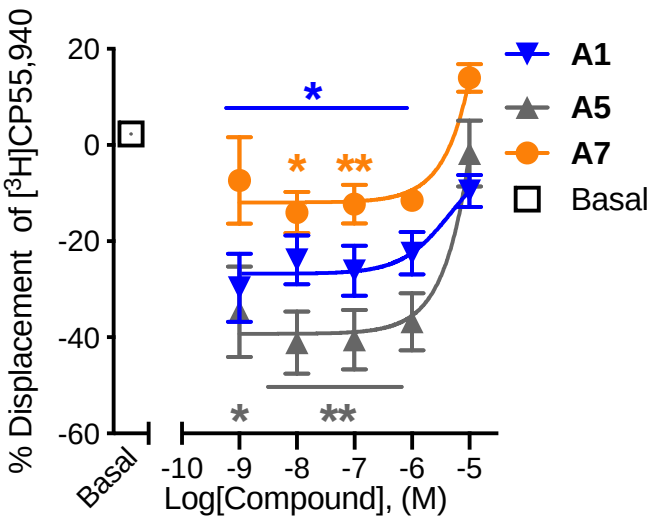

Figure 3. Effects of compounds **A1** (SV-10a, blue) **A5** (SB-13a, grey), **A7** (SB-16a, orange) at 1 nM - 10 μM on [^{3}H]CP55,940 binding to hCB2R. Asterisks indicate mean values significantly different from basal for each corresponding colour; *$p < 0.05$, **$p < 0.01$ relative to basal control as determined by one-way ANOVA followed by Bonferroni's *post-hoc* analysis. Data were fit to a nonlinear regression (4 parameter model, GraphPad v. 8). Data are expressed as the mean ± SEM of 4-6 independent experiments, each performed in duplicate.

In order to assess their selectivity for hCB2R relative to hCB1R, **A1** and **A5** were evaluated performing [^{3}H]CP55,940 binding experiments on CHO cells overexpressing hCB1R. The concentration binding curves (1 nM - 10 μM) displayed in Figure 4 indicate that **A1** and **A5** did not change [^{3}H]CP55,940 binding at hCB1R relative to basal levels of [^{3}H]CP55,940 binding at any concentrations tested. Therefore, the activity of these compounds are likely to be hCB2R-dependent between 1 nM and 10 μM. Although it is possible these allosteric ligands have non-specific effects at other, non-cannabinoid receptors, such experiments are beyond the scope of the present study. Based on the evidence gathered here that **A1** and **A5** enhanced binding of CP55,940 to CB2R, we chose to further evaluate these compound's functional activity at CB2R.

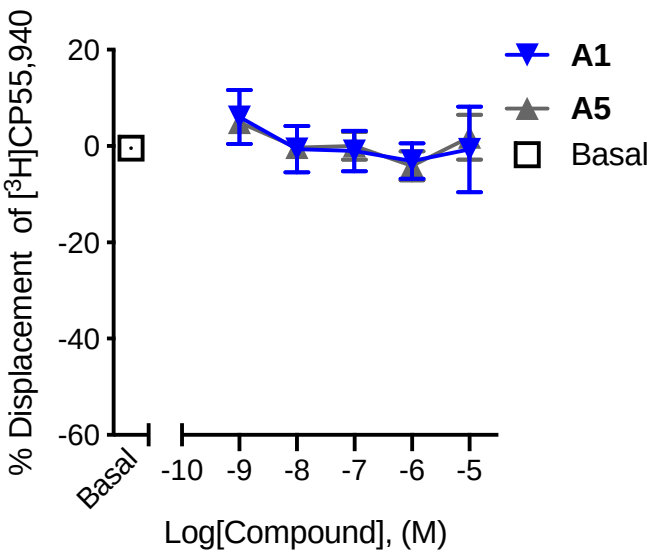

Figure 4. Effects of compounds **A1** (SV-10a, blue) and **A5** (SB-13a, grey) at 1 nM - 10 μM on [^{3}H]CP55940 binding to hCB1R. Data are expressed as the mean ± SEM of 6 independent experiments, each performed in duplicate.

2.2.3. [^{35}S]GTPγS Assay

To evaluate the functional activity of **A1** (SV-10a) and **A5** (SB-13a**)** on CB2R, both compounds (1 nM - 10 μM) were tested in the [^{35}S]GTPγS assay, carried out in the presence of [^{35}S]GTPγS (0.1 nM), GDP (30 μM), GTPγS (30 μM), with CHO cell membranes (1 mg/mL) overexpressing hCB2R. This was done in order to determine their ability to affect hCB2R functionality on their own (i.e. in the absence of CP55,940). This assay was performed in order to exclude the possibility that **A1** (SV-10a) and **A5** (SB-13a) do produce a functional effect by themselves, since this behavior would preclude their pure allosteric nature. **A5** (SB-13a) did not produce significant stimulation or inhibition of [^{35}S]GTPγS binding to hCB2Rs at the concentrations in which it was tested (Figure 5). **A1** (SV-10a) produced a slight decrease in [^{35}S]GTPγS binding at the highest concentrations tests, 1 and 10 μM, possibly indicating inverse agonist activity at these high concentrations for G protein binding when **A1** (SV-10a) is utilized in the absence of the probe orthosteric agonist, CP55,940.

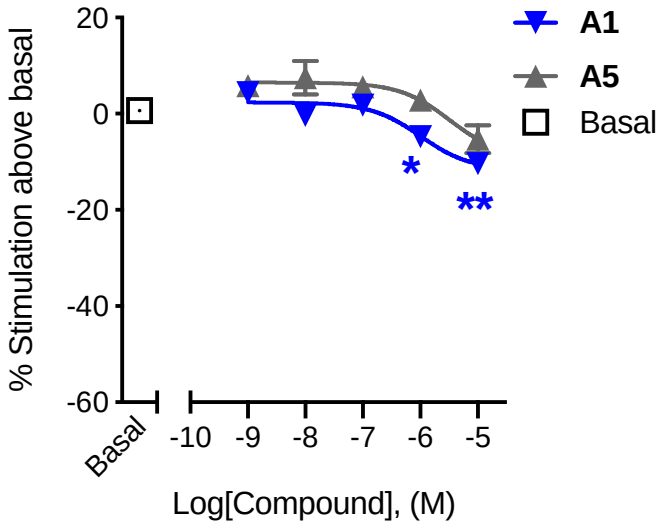

Figure 5. CB2R [^{35}S]GTPγS binding assays performed in the presence of **A1** (SV-10a) (blue) or **A5** (SB-13a) (grey) in the absence of the orthosteric ligand. Asterisks indicate mean values significantly different from basal for each corresponding colour; *$p < 0.05$, **$p < 0.01$ relative to basal control as determined by one-way ANOVA followed by Bonferroni's *post-hoc* analysis. Data were fit to a nonlinear regression (4 parameter model, GraphPad v. 8). Data are expressed as the mean ± SEM of 6 independent experiments, each performed in duplicate.

[^{35}S]GTPγS binding was repeated under the conditions above but in the presence of CP55,940 (1 nM - 10 μM). The potency of CP55,940 for its enhancement of [^{35}S]GTPγS binding to hCB2R was not significantly altered by 1 nM or 100 nM of either compound (Figure 6); however, a significant increase in E_{max} for both compounds was observed. This result suggests that, in addition to **A1** (SV-10a) and **A5** (SB-13a) enhancing the binding of [^{3}H]CP55,940 to hCB2R, **A1** and **A5** were also able to augment the efficacy, but not potency, of CP55,940-dependent hCB2R activation within the concentration range tested.

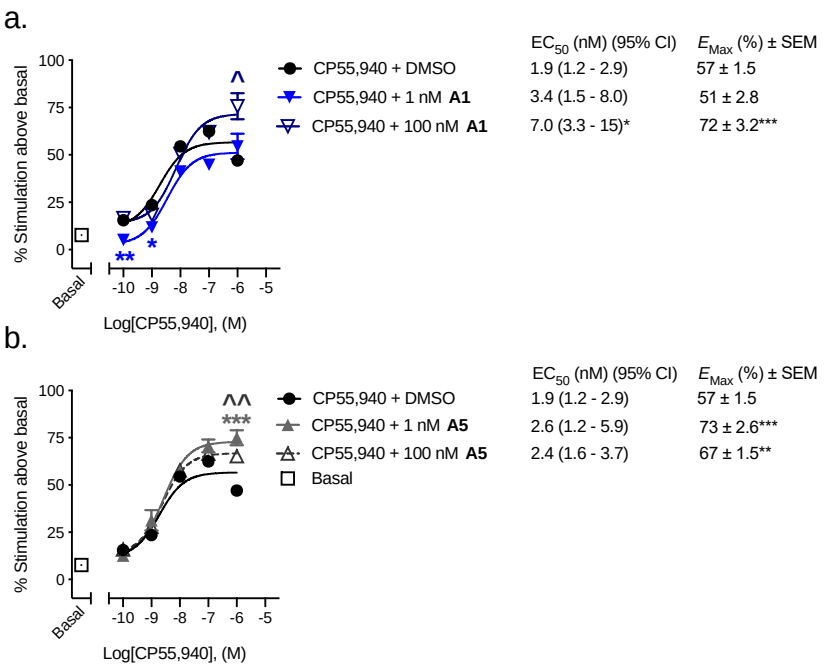

Figure 6. CB2R [^{35}S]GTPγS binding assays performed with CP55,940 and compound **A1** (SV-10a) (a, blue) or **A5** (SB-13a) (b, grey). Asterisks and carets in graphs indicate mean values significantly different from CP55,940 + DMSO control; *$p < 0.05$, **$p < 0.01$, ***$p < 0.001$ 1 nM compound relative to CP55,940 + DMSO; ^$p < 0.05$, ^^$p < 0.01$ 100 nM compound relative to CP55,940 + DMSO; as determined by one-way ANOVA followed by Bonferroni's *post-hoc* analysis. Asterisks in accompanying tables indicate mean values significantly different from CP55,940 + DMSO control; *$p < 0.05$, **$p < 0.01$, ***$p < 0.001$ compound relative to CP55,940 + DMSO as determined by non-overlapping 95% confidence intervals (EC_{50}) or one-way ANOVA followed by Bonferroni's *post-hoc* analysis (E_{max}). Data were fitted to a nonlinear regression (4 parameter model, GraphPad v. 8). All data are expressed as the mean ± SEM of 6 independent experiments each performed in duplicate, with the exception of EC_{50}, which is expressed as mean with 95% confidence intervals.

2.2.4. Inhibition of forskolin-stimulated cAMP

Following our initial [^{3}H]CP55,940 binding and [^{35}S]GTPγS assessments, **A1** (SV-10a), **A5** (SB-13a) and the parent compound **EC21a**, were characterized for $G\alpha_{i/o}$ protein-dependent inhibition of forskolin (FSK)-stimulated cAMP accumulation in CHO cells stably-expressing hCB2R. Cells were treated with 10 μM FSK and CP55,490 or 10 nM CP55,940 + compound for 90 min to assess compound concentration-dependent PAM activity in the presence of CP55,940 (Figure 7a). Ten nM CP55,940 was used for the orthosteric ligand because CP55,940 alone at 10 nM produced an approximately 50% response in the assay; allowing us to observe changes in the cAMP response produced following co-incubation with varying concentrations of our PAMs as we have done

previously [8]. In this way, the CP55,940 data represent an internal control for these experiments. Concentration-response curves with **EC21a**, **A1** (SV-10a), and **A5** (SB-13a) begin approximately 50% above the baseline because of co-incubation with 10 nM CP55,940. The parent compound, **EC21a** augmented 10 nM CP55,940-dependent signalling to yield maximum hCB2R activation (E_{max} = 91 ± 6.9%) consistent with the expected activity of a PAM and with a potency of 3.8 (0.29 – 57) nM. **A1** (SV-10a) also augmented 10 nM CP55,940-dependent signalling to yield maximum observed hCB2R activation (E_{max} = 120 ± 22% at 10 µM) consistent with the expected activity of a PAM, albeit with very low potency (> 10,000 nM) that could not be accurately estimated without a plateau for this curve. Similar to the parent compound, **A5** (SB-13a), augmented 10 nM CP55,940-dependent signalling to yield maximum hCB2R activation (E_{max} = 101 ± 6.9%) consistent with positive allosteric modulation and with a potency that was not different to that of **EC21a** 15 (2.4 – 90) nM. Therefore, all compounds tested were PAMs of CP55,940- and hCB2R-dependent cAMP inhibition.

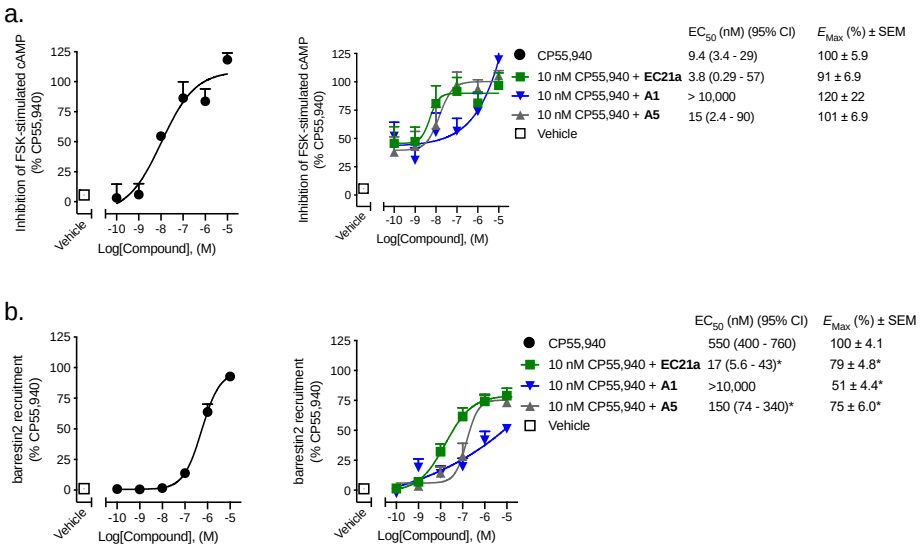

Figure 7. CHO cells stably-expressing hCB2R were treated with 0.10 nM – 10 µM CP55,940 or 0.10 nM – 10 µM compound + 10 nM CP55,940 for 90 min and cAMP inhibition (a) or βarrestin2 recruitment was measured (b). cAMP data are expressed as % inhibition of FSK-stimulated cAMP response relative to the maximum response for CP55,940. βarrestin2 recruitment data are expressed as % CP55,940 response. Asterisks in accompanying tables indicate mean values significantly different from CP55,940 control; *$p < 0.05$ compound relative to CP55,940 as determined by non-overlapping 95% confidence intervals (EC_{50}) or one-way ANOVA followed by Bonferroni's *post-hoc* analysis (E_{max}). Data were fitted to a nonlinear regression (4 parameter model, GraphPad v. 8). Data are mean values ± S.E.M. or 95% CI (EC_{50}), of 6 independent experiments performed in triplicate.

2.2.5. Recruitment of βarrestin2

In addition to G protein-mediated signalling, G protein-coupled receptors also interact with βarrestins, which facilitate receptor internalization, recycling, degradation, and signalling. **EC21a**, **A1** (SV-10a), and **A5** (SB-13a) were evaluated for their ability to enhance CP55,940-dependent βarrestin2 recruitment in CHO cells stably-expressing hCB2R. Cells were treated with CP55,490 or 10 nM CP55,940 + compound for 90 min (Figure 7b). Ten nM CP55,940 was chosen in these assays to keep experimental conditions consistent with those of cAMP inhibition data presented in figure 7a. The parent compound, **EC21a**, augmented 10 nM CP55,940-dependent signalling to yield sub-maximal hCB2R βarrestin2 recruitment (E_{max} = 79 ± 4.8%) consistent with PAM activity [EC_{50} = 17 (5.6 – 43) nM]. Although the observed E_{max} was not greater than the orthosteric agonist CP55,940 alone at 10 μM, **EC21a** did increase barrestin2 recruitment in the presence of 10 nM CP55,940 above the effect produced by 10 nM CP55,940 alone. **A1** (SV-10a) weakly enhanced βarrestin2 recruitment [E_{max} = 51 ± 4.4% at 10 μM; EC_{50} > 10,000 nM (i.e. beyond the concentration range used in these experiments)]. **A5** (SB-13a) also enhanced 10 nM βarrestin2 recruitment to hCB2R with less potency than the parent compound [E_{max} = 75 ± 6.0%; EC_{50} = 150 (74 – 340) nM]. Therefore, all compounds tested were also PAMs of CP55,940- and hCB2R-dependent βarrestin2 recruitment. However, a consistent trend for all compounds was that their potency and efficacy were greater in the inhibition of cAMP assay than the βarrestin2 recruitment assay.

In G protein-binding experiments, we had observed **A1** (SV-10a) and **A5** (SB-13a) did not increase GTPγS binding at 10 nM CP55,940 and 100 nM compound (Figure 6). In contrast, this combination of 10 nM CP55,940 and 100 nM compound produced an approximately 50% increase in both inhibition of cAMP accumulation (Figure 7a) and βarrestin2 recruitment (Figure 7b). These differences between G protein-binding that occurs proximal to the receptor and the signaling assays that measure multiple events following ligand binding are likely the result of signal amplification that occurs downstream of G protein coupling, and are therefore more sensitive as has been documented

previously [17]. Moreover, these data speak to ligand-specific effects that vary between signaling endpoints and underscore the importance of measuring different ligand-dependent outomces [8,11].

3. Conclusions

Modulation of the CB2R is an interesting approach for pain and inflammation, arthritis, addictions, neuroprotection, and cancer, among other possible therapeutic applications. However, the use of CB2R orthosteric agonists has shown several disadvantages, limiting their usefulness as clinically relevant drugs. This disadvantage is probably because of the predominance of CB2R on immune cells whose activation might cause immunosuppression. Furthermore, several studies have reported that CB2R agonists can induce internalization and desensitization of the receptor leading to a decrease in signalling and surface receptor levels [29]. PAMs represent a promising approach to achieving the potential therapeutic benefits of orthosteric CB2R agonists limiting their adverse effects. Indeed, PAMs have no intrinsic efficacy and enhance receptor activation only in the presence of the orthosteric agonist, allowing improved regulation with no or reduced receptor desensitisation [19, 30].

In this work we reported the design, synthesis, and biological evaluation of 18 new derivatives of the known CB2R PAM, **EC21a**, recently discovered by us [10]. The obtained results indicated that compounds **A1** (SV-10a) and **A5** (SB-13a) behaved as CB2R PAMs as indicated by their ability, at 1 nM to 1 μM, to produce increases in the binding of [^{3}H]CP55940 to CB2Rs. As expected for an allosteric modulator, both compounds did not independently activate CB2R in the [^{35}S]GTPγS assay, in the absence of a CB2R agonist. At 100 nM and 1 nM, **A1** (SV-10a) and **A5** (SB-13a) enhanced the efficacy but not the potency with which CP55,940 stimulates [^{35}S]GTPγS binding to CB2Rs. Finally, **A1** (SV-10a), **A5** (SB-13a) and the parent compound **EC21a** modulated CP55,940-dependent βarrestin2 recruitment and cAMP inhibition. In particular, their potency and efficacy were greater in the inhibition of cAMP assay than the βarrestin2 recruitment assay.

Although only compounds **A1** and **A5** were found to have allosteric behavior on CB2R, the obtained results enable to extend the structural-activity relationships of these type of molecules for interaction with the CB2R allosteric site. First of all, the presence of an aliphatic substituent at position 1 is detrimental for allosteric activity, maybe because of the loss of some specific interactions (e.g. π-π stacking). However, the lack of allosteric behavior on CB2R of the unsubstituted benzyl derivative **A3** indicates that specific stereo-electronic requirements have also to be satisfied and that are peculiar of compounds **EC21a**, **A1** and **A5** characterized by fluorine atom or by chlorine atom in para or ortho position of the phenyl group. Furthermore, the cycloheptane-carboxamide at position 3 seems to be directly engaged in the interaction with the allosteric site of CB2R, indeed its substitution with other aliphatic or aromatic carboxamides or its replacement with different functional groups abolished all evidence of allosteric activity.

These findings might be useful for the characterization of an allosteric binding pocket whose existence close to the CB2R orthosteric binding site was recently suggested [31-32].

4. Experimental Section

4.1. Chemistry

Commercially available reagents were purchased from Sigma Aldrich, Tokyo Chemical Industry or Fluorochem and used without purification. ^{1}H-NMR and ^{13}C-NMR were recorded at 400 and 100 MHz respectively, on a Bruker AVANCE IIITM 400 spectrometer. Chemical shift (δ) are reported in parts per million related to the residual solvent signal, while coupling constants (*J*) are expressed in Hertz (Hz). Microwave-assisted reactions were run in a Biotage® Initiator + microwave synthesizer.

Isolera™ Prime – Biotage was used for the purification of some derivatives. All final compounds were analyzed by HPLC, showing a purity ≥ 95%. A Bechman HPLC instrument equipped with a System Gold Solvent Delivery module (Pumps) 125, System Gold UV/ VIS Detector 166, Detector set to 280 nm, was employed. Analyses were performed on a reverse phase C18 column (Phenomenex

250 × 4.6 mm, 5mm particle size, Gemini). The mobile phase was constituted by a mixture of H_2O/AcOH (0.1% v/v) (eluent A) and ACN (eluent B). A gradient starting from 50% of B, changing to 100% of B over 20min, and returning to the initial conditions over 10 min, was used for compounds. The flow rate was 1.0 mL/min. High-resolution mass spectra (HRMS) were recorded on a Q Exactive™ Plus Hybrid Quadrupole-Orbitrap™ Mass Spectrometer (Thermo Fisher Scientific), equipped with HESI source. The ESI-MS spectrum was recorded by direct injection at 5 μl min−1 flow rate. Working conditions: positive polarity, spray voltage 3.5 kV, capillary temperature 300 °C, S-lens RF level 55, sheath gas 20, auxiliary gas 3 (arbitrary units); negative polarity, spray voltage 3.4 kV, capillary temperature 270 °C, S-lens RF level 55, sheath gas 35, auxiliary gas 8 (arbitrary units). Acquisition and analysis: Xcalibur 4.2 software (Thermo). For spectra acquisition a nominal resolution (at m/z 200) of 140000 was used. Organic solutions were dried over anhydrous Na_2SO_4. Evaporation was carried out in vacuo using a rotating evaporator. Silica gel flash chromatography was performed using silica gel 60 Å (0.040–0.063 mm; Merck Life Science S.r.l.). Reactions was monitored by TLC on Merck aluminium silica gel (60 F_{254}) plates that were visualized under a UV lamp (λ = 254 nm). Melting points were determined on a Kofler hot-stage apparatus and are uncorrected.

4.1.1. General procedure for the synthesis of compounds ***1-9***

NaH (60% dispersion in mineral oil) (0.156 g, 6.49 mmol) was added portion wise at 0°C to a solution of the commercial available 2-hydroxy-4-methyl-3-nitropyridine (1.00 g, 6.49 mmol) in DME (29 mL) and anhydrous DMF (7.2 mL). LiBr (1.13 g, 12.98 mmol) was added 10 minutes later. The mixture was stirred for 15 min at room temperature. The suitable benzyl chloride (12.98 mmol) was added dropwise and the reaction was stirred at 65 °C overnight. Solvents were removed under reduced pressure. The mixture obtained was dissolved in $CHCl_3$ and washed three times with water. The organic phase was dried over Na_2SO_4, filtered and evaporated under reduced pressure.

*4.1.1.1. 1-(4-fluorobenzyl)-4-methyl-3-nitropyridin-2(1H)-one (**1**).*

Ocher oil (1.70 g, 6.47 mmol, Yield: > 99 %). ^{1}H-NMR ($CDCl_3$) δ: 7.33, 7.04 (AA'XX' system, 4H, Ar-*H*), 7.29 (d, 1H, *J*= 7.2 Hz, H_6-Py), 6.08 (d, 1H, *J*= 7.2 Hz, H_5-Py), 5.12 (s, 2H, PhCH_2N), 2.26 (s, 3H, CH_3-Py).

*4.1.1.2. 1-(2-fluorobenzyl)-4-methyl-3-nitropyridin-2(1H)-one (**2**).*

Purification by flash column chromatography (1:1 hexane- ethyl acetate). Brown solid (1.34 g, 5.13 mmol, Yield: 79 %). ^{1}H-NMR ($CDCl_3$) δ: 7.52-7.50 (m, 1H, Ar-*H*), 7.47 (d, 1H, *J* = 7.5 Hz, H_6-Py), 7.45-7.29 (m, 1H, Ar-*H*); 7.16-7.05 (m, 2H, Ar-*H*), 6.08 (d, 1H, *J* =7.5 Hz, H_5-Py), 5.16 (s, 2H, PhCH_2N); 2.24 (s, 3H, CH_3-Py).

*4.1.1.3. 1-(3-fluorobenzyl)-4-methyl-3-nitropyridin-2(1H)-one (**3**).*

Purification by flash column chromatography (1:1 hexane-ethyl acetate). Beige solid (1.07 g, 4.09 mmol, Yield: 63 %). ^{1}H-NMR ($CDCl_3$) δ: 7.35-7.31 (m, 1H, Ar-*H*), 7.30 (d, 1H, *J* = 8 Hz, H_6-Py), 7.11-7.09 (m, 1H, Ar-*H*), 7.06-7.01 (m, 2H, Ar-*H*), 6.10 (d, 1H, *J* = 8 Hz, H_5-Py), 5.14 (s, 2H, PhCH_2N), 2.27 (s, 3H, CH_3-Py).

*4.1.1.4. 1-benzyl-4-methyl-3-nitropyridin-2(1H)-one (**4**).*

Purification by flash column chromatography (6:4 hexane- ethyl acetate). Brown solid (0.935 g, 3.83 mmol, Yield: 59 %). ^{1}H-NMR ($CDCl_3$) δ: 7.37-7.29 (m, 6H, Ar-*H,* H_6-Py), 6.07 (d, 1H, *J* = 7.2 Hz, H_5-Py), 5.15 (s, 2H, PhCH_2N), 2.25 (s, 3H, CH_3-Py).

*4.1.1.5. 1-(4-chlorobenzyl)-4-methyl-3-nitropyridin-2(1H)-one (**5**).*

Purification by flash column chromatography (6:4 hexane-ethyl acetate). Brown solid (0.995 g, 3.57 mmol, Yield: 55 %). ^{1}H-NMR ($CDCl_3$) δ: 7.35-7.33 (m, 2H, Ar-*H*), 7.29-7.26 (m, 3H, Ar-*H,* H_6-Py), 6.09 (d, 1H, *J* = 7.2 Hz, H_5-Py), 5.12 (s, 2H, PhCH_2N), 2.26 (s, 3H, CH_3-Py).

*4.1.1.6. 1-(2-chlorobenzyl)-4-methyl-3-nitropyridin-2(1H)-one (**6**).*

Purification by flash column chromatography (1:1 hexane-ethyl acetate). Brown solid (1.75 g, 6.30 mmol, Yield: 97 %). ^{1}H-NMR ($CDCl_3$) δ: 7.46-7.30 (m, 2H, Ar-*H*), 7.41 (d, 1H, *J* = 7.2 Hz, H_6-Py), 7.31-7.27 (m, 2H, Ar-*H*), 6.09 (d, 1H, *J* = 7.2 Hz, H_5-Py), 5.28 (s, 2H, PhCH_2N), 2.27 (s, 3H, CH_3-Py).

*4.1.1.7. 1-(4-iodobenzyl)-4-methyl-3-nitropyridin-2(1H)-one (**7**).*

Purification by flash column chromatography (6:4 hexane-ethyl acetate). Brown solid (2.33 g, 6.30 mmol, Yield: 97 %). ^{1}H-NMR ($CDCl_3$) δ: 7.70, 7.08 (AA'XX' system, 4H, Ar-*H*), 7.28 (d, 1H, *J* = 7.2 Hz, H_6-Py), 6.08 (d, 1H, *J* = 7.2 Hz, H_5-Py), 5.09 (s, 2H, PhCH_2N), 2.26 (s, 3H, CH_3-Py).

*4.1.1.8. 1-(4-bromobenzyl)-4-methyl-3-nitropyridin-2(1H)-one (**8**).*

Purification by flash column chromatography (1:1 hexane-ethyl acetate). Brown solid (0.881 g, 2.73 mmol, Yield: 42 %). ^{1}H-NMR ($CDCl_3$) δ: 7.50, 7.21 (AA'XX' system, 4H, Ar-*H*), 7.28 (d, 1H, *J* = 7.2 Hz, H_6-Py), 6.08 (d, 1H, *J* = 7.2 Hz, H_5-Py), 5.10 (s, 2H, PhCH_2N), 2.26 (s, 3H, CH_3-Py).

*4.1.1.9. 1-(2-morpholinoethyl)-4-methyl-3-nitropyridin-2(1H)-one (**9**).*

Purification by flash column chromatography (9:1 ethyl acetate-methanol). Yellow oil (0.347 g, 1.30 mmol, Yield: 20 %). ^{1}H-NMR ($CDCl_3$) δ: 7.36 (d, 1H, *J* = 6.8 Hz, H_6-Py), 6.08 (d, 1H, *J* = 6.8 Hz, H_5-Py), 4.06 (t, 2H, *J* = 6.0 Hz, CH_2NCO), 3.68-3.65 (m, 4H, 2×CH_2O); 2.69 (t, 2H, *J* = 6.0 Hz, CH_2CH$_2$NCO), 2.51-2.48 (m, 4H, 2×CH_2N), 2.27 (s, 3H, CH_3-Py).

*4.1.2. General procedure for the synthesis of compounds **10-18**, **34** and **B8***

Compound **1-9** (1.94 mmol), iron powder (1.35 g, 24.19 mmol) and ammonium chloride (0.683 g, 12.77 mmol) were added to a solution of water (10.14 mL) and ethanol (20.28 mL). The mixture was

refluxed at 80 °C for 3 h, filtered under vacuum and evaporated under reduced pressure. The solid obtained was dissolved in $CHCl_3$ and washed with water. The organic phase was dried over Na_2SO_4, filtered and evaporated under reduced pressure.

*4.1.2.1. 3-amino-1-(4-fluorobenzyl)-4-methylpyridin-2(1H)-one (**10**).*

Ocher solid (0.448 g, 1.93 mmol, Yield: > 99 %). ^{1}H-NMR: ($CDCl_3$) δ: 7.26, 7.00 (AA'XX' system, 4H, Ar-*H*), 6.70 (d, 1H, *J* = 6.8 Hz, H_6-Py), 5.99 (d, 1H, *J* = 6.8 Hz, H_5-Py), 5.11 (s, 2H, PhCH_2N), 3.10 (bs, 2H, NH_2), 2.05 (s, 3H, CH_3-Py).

*4.1.2.2. 3-amino-1-(2-fluorobenzyl)-4-methylpyridin-2(1H)-one (**11**)*

Purification by flash column chromatography (4:6 hexane-ethyl acetate). Beige oil (0.301 g, 1.30 mmol, Yield: 67 %). ^{1}H-NMR ($CDCl_3$) δ: 7.37-7.33 (m, 1H, Ar-*H*), 7.27-7.25 (m, 1H, Ar-*H*), 7.10-7.03 (m, 2H, Ar-*H*), 6.78 (d, 1H, *J* = 6.8 Hz, H_6-Py), 5.99 (d, 1H, *J* = 6.8 Hz, H_5-Py), 5.19 (s, 2H, PhCH_2N), 4.08 (bs, 2H, NH_2), 2.04 (s, 3H, CH_3-Py).

*4.1.2.3. 3-amino-1-(3-fluorobenzyl)-4-methylpyridin-2(1H)-one (**12**).*

Purification by flash column chromatography (4:6 hexane-ethyl acetate). Beige oil (0.378 g, 1.63 mmol, Yield: 84 %). ^{1}H-NMR ($CDCl_3$) δ: 7.29-7.27 (m, 1H, Ar-*H*), 7.05-7.03 (m, 1H, Ar-*H*), 6.96-6.93 (m, 2H, Ar-*H*), 6.69 (d, 1H, *J* = 6.8 Hz, H_6-Py), 6.01 (d, 1H, *J* = 6.8 Hz, H_5-Py), 5.14 (s, 2H, PhCH_2N), 3.87 (bs, 2H, NH_2), 2.06 (s, 3H, CH_3-Py).

*4.1.2.4. 3-amino-1-benzyl-4-methylpyridin-2(1H)-one (**13**).*

Purification by flash column chromatography (6:4 hexane-ethyl acetate). Brown solid (0.245 g, 1.14 mmol, Yield: 59 %). ^{1}H-NMR ($CDCl_3$) δ: 7.34-7.27 (m, 5H, Ar-*H*), 6.71 (d, 1H, *J* = 7.2 Hz, H_6-Py), 5.99 (d, 1H, *J* = 7.2 Hz, H_5-Py), 5.16 (s, 2H, PhCH_2N), 4.10 (bs, 2H, NH_2), 2.07 (s, 3H, CH_3-Py).

*4.1.2.5. 3-amino-1-(4-chlorobenzyl)-4-methylpyridin-2(1H)-one (**14**).*

Purification by flash column chromatography (6:4 hexane-ethyl acetate). Brown solid (0.265 g, 1.07 mmol, Yield: 55 %). ^{1}H-NMR ($CDCl_3$) δ: 7.28, 7.21 (AA'XX' system, 4H, Ar-*H*), 6.67 (d, 1H, *J* = 7.2 Hz, H_6-Py), 5.99 (d, 1H, *J* = 7.2 Hz, H_5-Py), 5.10 (s, 2H, PhCH_2N), 4.11 (bs, 2H, NH_2), 2.04 (s, 3H, CH_3-Py).

*4.1.2.6. 3-amino-1-(2-chlorobenzyl)-4-methylpyridin-2(1H)-one (**15**).*

Purification by flash column chromatography (6:4, hexane-ethyl acetate). Brown solid (0.468 g, 1.88 mmol, Yield: 97 %). ^{1}H-NMR ($CDCl_3$) δ:7.46-7.42 (m, 1H, Ar-*H*), 7.25-7.18 (m, 2H, Ar-*H*), 7.13-7.11 (m, 1H, Ar-*H*), 6.71 (d, 1H, *J* = 7.2 Hz, H_6-Py), 6.01 (d, 1H, *J* = 7.2 Hz, H_5-Py), 5.27 (s, 2H, PhCH_2N), 4.12 (bs, 2H, NH_2), 2.07 (s, 3H, CH_3-Py).

*4.1.2.7. 3-amino-1-(4-iodobenzyl)-4-methylpyridin-2(1H)-one (**16**).*

Purification by flash column chromatography (6:4 hexane-ethyl acetate). Brown solid (0.640 g, 1.88 mmol, Yield: 97 %). ^{1}H-NMR ($CDCl_3$) δ:7.67, 7.05 (AA'XX' system, 4H, Ar-*H*), 6.69 (d, 1H, *J* = 7.2 Hz, H_6-Py), 6.02 (d, 1H, *J* = 7.2 Hz, H_5-Py), 5.10 (s, 2H, PhCH_2N), 4.12 (bs, 2H, NH_2), 2.08 (s, 3H, CH_3-Py).

*4.1.2.8. 3-amino-1-(4-bromobenzyl)-4-methylpyridin-2(1H)-one (**17**).*

Purification by flash column chromatography (1:1 hexane-ethyl acetate). Brown solid (0.239 g, 0.815 mmol, Yield: 42 %). ^{1}H-NMR ($CDCl_3$) δ:7.44, 7.15 (AA'XX' system, 4H, Ar-*H*), 6.67 (d, 1H, *J* = 7.2 Hz, H_6-Py), 5.99 (d, 1H, *J* = 7.2 Hz, H_5-Py), 5.10 (s, 2H, PhCH_2N), 4.10 (bs, 2H, NH_2), 2.05 (s, 3H, CH_3-Py).

*4.1.2.9. 3-amino-1-(2-morpholinoethyl)-4-methylpyridin-2(1H)-one (**18**).*

Purification by flash column chromatography (1:1 hexane-ethyl acetate). Brown solid (0.193 g, 0.815 mmol, Yield: 42 %). ^{1}H-NMR ($CDCl_3$) δ: 6.66 (d, 1H, *J* = 7.0 Hz, H_6-Py), 5.94 (d, 1H, *J* = 7.0 Hz, H_5-Py), 4.03-4.00 (m, 4H, CH_2NCO, NH_2), 3.66-3.63 (m, 4H, 2×CH_2O), 2.65 (t, 2H, *J* = 6.8 Hz, CH_2CH$_2$NCO), 2.49-2.46 (m, 4H, 2×CH_2N), 2.01 (s, 3H, CH_3-Py).

*4.1.2.10. 3-amino-4-methylpyridin-2(1H)-one (**33**).*

Brown solid (0.236 g, 1.90 mmol, Yield: 98 %). ^{1}H-NMR ($CDCl_3$) δ: 6.77 (d, 1H, *J* = 6.8 Hz, H_6-Py), 6.09 (d, 1H, *J* = 6.8 Hz, H_5-Py), 2.84 (bs, 2H, NH_2), 2.10 (s, 3H, CH_3-Py).

*4.1.2.11. 3-amino-5-bromo-1-(4-fluorobenzyl)-4-methylpyridin-2(1H)-one (**B8**)*

Trituration in Et_2O. Grey solid (0.422 g, 1.36 mmol, Yield: 70 %). Mp: 92-95 °C. ^{1}H-NMR ($CDCl_3$) δ:7.30-7.26 (m, 2H, Ar-*H*), 7.05-7.00 (m, 3H, Ar-*H*, H_6-Py), 5.09 (s, 2H, PhCH_2N), 2.20 (s, 3H, CH_3-Py). ^{13}C-NMR ($CDCl_3$) δ (ppm): 162.62 (d, $J_{C\text{-}F}$= 245 Hz, Ar-*C*F); 156.13 (*C*$_2$-Py), 146.92 (*C*$_3$-Py), 135.55 (*C*$_4$-Py), 132.00 (d, $J_{C\text{-}F}$= 3 Hz, Ar-*C*), 130.01 (d, $J_{C\text{-}F}$= 9 Hz, 2×Ar-*C*H), 123.81 (*C*$_6$-Py),115.90 (d, $J_{C\text{-}F}$= 22 Hz, 2×Ar-*C*H), 104.87 (*C*$_5$-Py), 51.78 (Ph*C*H$_2$N), 16.66 (*C*H$_3$-Py). HRMS-ESI: m /z calcd for $C_{13}H_{12}BrFN_2O$ $[M+H]^+$, 311.01898; found 311.01862.

*4.1.3. General procedure for the synthesis of compounds **19-26, 30, 34.***

Cycloheptane carboxylic acid (0.86 mL, 6.29 mmol) was dissolved in $C_2O_2Cl_2$ (1.59 mL, 18.87 mmol) and 3 drops of DMF, in a vial under nitrogen. The solution was stirred at room temperature for 30 min to allow the production of acyl chloride. Then the excess of $C_2O_2Cl_2$ was removed by evaporation under nitrogen flux. In the meantime, compound **10-18** (4.71 mmol) was dissolved in anhydrous DMF, and then triethylamine (3.18 mL, 23.56 mmol) was added. This latter solution was added dropwise, under nitrogen and at 0 °C, to the solution of acyl chloride previously prepared. Reaction mixture was stirred at room temperature for 24 h. DMF was removed under reduced pressure. The residue obtained was dissolved in $CHCl_3$ and washed three times with a solution of 5%

HCl. The organic phase was dried over Na_2SO_4, filtered and evaporated under reduced pressure to give a brown oil.

*4.1.3.1. N-(1-(2-fluorobenzyl)-4-methyl-2-oxo-1,2-dihydropyridin-3-yl)-cycloheptane-carboxamide (**19**).*

Purification by Isolera™ Prime – Biotage chromatography (1:1 hexane-ethyl acetate). Brown solid (0.940 g, 2.64 mmol, Yield: 56 %). ^{1}H-NMR ($CDCl_3$) δ: 7.54 (bs, 1H, NH); 7.39-7.36 (m, 1H, Ar-*H*), 7.30-7.27 (m, 1H, Ar-*H*), 7.16 (d, 1H, *J* = 7.2 Hz, H_6-Py), 7.14-7.03 (m, 2H, Ar-*H*), 6.10 (d, 1H, *J*= 7.2 Hz, H_5-Py), 5.14 (s, 2H, PhCH_2N), 2.50-2.49 (m, 1H, C*H*CO), 2.11 (s, 3H, CH_3-Py), 2.03-1.99 (m, 2H, CH_2), 1.81-1.70 (m, 4H, 2×CH_2), 1.59-1.48 (m, 6H, 3×CH_2).

*4.1.3.2. N-(1-(3-fluorobenzyl)-4-methyl-2-oxo-1,2-dihydropyridin-3-yl)-cycloheptane-carboxamide (**20**)*

Purification by Isolera™ Prime – Biotage chromatography (1:1 hexane-ethyl acetate). Brown solid (1.09 g, 3.06 mmol, Yield: 65 %). ^{1}H-NMR ($CDCl_3$) δ: 7.44 (bs, 1H, NH), 7.31-7.26 (m, 1H, Ar-*H*), 7.04 (d, 1H, *J* = 7.2 Hz, H_6-Py), 7.02-6.96 (m, 3H, Ar-*H*),6.12 (d, 1H, *J* = 7.2 Hz, H_5-Py), 5.09 (s, 2H, PhCH_2N), 2.52-2.47 (m, 1H, C*H*CO), 2.13 (s, 3H, CH_3-Py), 2.06-2.00 (m, 2H, CH_2), 1.82-1.74 (m, 4H, 2×CH_2), 1.65-1.49 (m, 6H, 3×CH_2).

*4.1.3.3. N-(1-benzyl-4-methyl-2-oxo-1,2- dihydropyridin-3-yl)-cycloheptane-carboxamide (**21**).*

Purification by flash column chromatography (3:7 hexane-ethyl acetate). Brown solid (0.749 g, 2.21 mmol, Yield: 47 %). ^{1}H-NMR ($CDCl_3$) δ: 7.50 (bs, 1H, NH), 7.36-7.27 (m, 5H, Ar-*H*), 7.04 (d, 1H, *J* = 7.2 Hz, H_6-Py), 6.09 (d, 1H, *J* = 7.2 Hz, H_5-Py), 5.11 (s, 2H, PhCH_2N), 2.52-2.47 (m, 1H, C*H*CO), 2.12 (s, 3H, CH_3-Py), 2.06-2.00 (m, 2H, CH_2), 1.81-1.72 (m, 4H, 2×CH_2), 1.59-1.46 (m, 6H, 3×CH_2).

*4.1.3.4. N-(1-(4-chlorobenzyl)-4-methyl-2-oxo-1,2-dihydropyridin-3-yl)-cycloheptane-carboxamide **(22)**.*

Purification by flash column chromatography (1:1 hexane-ethyl acetate). Brown solid (0.141 g, 0.377 mmol, Yield: 8 %). ^{1}H-NMR ($CDCl_3$) δ: 7.43 (bs, 1H, NH), 7.31, 7.21 (AA'XX' system, 4H, Ar-*H*), 7.03 (d, 1H, *J* = 7.2 Hz, H_6-Py), 6.11 (d, 1H, *J* = 7.2 Hz, H_5-Py), 5.07 (s, 2H, PhCH_2N), 2.52-2.46 (m, 1H, C*H*CO), 2.13 (s, 3H, CH_3-Py), 2.05-2.00 (m, 2H, CH_2), 1.80-1.74 (m, 4H, 2×CH_2), 1.57-1.47 (m, 6H, 3×CH_2).

*4.1.3.5. N-(1-(2-chlorobenzyl)-4-methyl-2-oxo-1,2-dihydropyridin-3-yl)-cycloheptane-carboxamide **(23)**.*

Purification by flash column chromatography (4:6 hexane-ethyl acetate). Brown solid (0.615 g, 1.65 mmol, Yield: 35 %). ^{1}H-NMR ($CDCl_3$) δ: 7.57 (bs, 1H, NH), 7.40-7.38 (m, 1H, Ar-*H*), 7.25-7.20 (m, 3H, Ar-*H*), 7.10 (d, 1H, *J* = 7.2 Hz, H_6-Py), 6.12 (d, 1H, *J* = 7.2 Hz, H_5-Py), 5.23 (s, 2H, PhCH_2N), 2.54-2.47 (m, 1H, C*H*CO), 2.13 (s, 3H, CH_3-Py), 2.02-1.98 (m, 2H, CH_2), 1.79-1.69 (m, 4H, 2×CH_2), 1.58-1.44 (m, 6H, 3×CH_2).

*4.1.3.6. N-(1-(4-iodobenzyl)-4-methyl-2-oxo-1,2-dihydropyridin-3-yl)-cycloheptane-carboxamide **(24)**.*

Purification by flash column chromatography (1:1 hexane-ethyl acetate). Brown solid (0.766 g, 1.65 mmol, Yield: 35 %). ^{1}H-NMR ($CDCl_3$) δ: 7.67-7.64 (m, 2H, Ar-*H*), 7.49 (bs, 1H, NH), 7.03-7.00 (m, 3H, Ar-*H,* H_6-Py), 6.11 (d, 1H, *J* = 7.2 Hz, H_5-Py), 5.04 (s, 2H, PhCH_2N), 2.52-2.48 (m, 1H, C*H*CO), 2.12 (s, 3H, CH_3-Py), 2.03-2.00 (m, 2H, CH_2), 1.81-1.68 (m, 4H, 2×CH_2), 1.59-1.41 (m, 6H, 3×CH_2).

*4.1.3.7. N-(1-(4-bromobenzyl)-4-methyl-2-oxo-1,2-dihydropyridin-3-yl)-cycloheptane carboxamide **(25)***

Purification by flash column chromatography (1:9 hexane-ethyl acetate). Brown solid (0.393 g, 0.942 mmol, Yield: 20 %). ^{1}H-NMR ($CDCl_3$) δ: 7.54 (bs, 1H, NH), 7.46, 7.15 (AA'XX' system, 4H, Ar-*H*), 7.03 (d, 1H, *J* = 7.0 Hz, H_6-Py), 6.11 (d, 1H, *J* = 7.0 Hz, H_5-Py), 5.05 (s, 2H, PhCH_2N), 2.53-2.48 (m, 1H, C*H*CO), 2.12 (s, 3H, CH_3-Py), 2.02-1.95 (m, 2H, CH_2), 1.77-1.71 (m, 4H, 2×CH_2), 1.58-1.44 (m, 6H, 3×CH_2).

*4.1.3.8. N-(1-(2-morpholinoethyl)-4-methyl-2-oxo-1,2-dihydropyridin-3-yl)-cycloheptane-carboxamide (**26**).*

Purification by flash column chromatography (8:2 ethyl acetate-methanol + 1 % Et_3N). Brown oil (0.749 g, 2.07 mmol, Yield: 44 %). ^{1}H-NMR ($CDCl_3$) δ: 7.39 (bs, 1H, NH), 7.04 (d, 1H, *J* = 6.8 Hz, H_6-Py), 6.07 (d, 1H, *J* = 6.8 Hz, H_5-Py) 4.01 (t, 2H, *J* = 6.6 Hz, CH_2NCO), 3.69-3.66 (m, 4H, 2×CH_2O), 2.65 (t, 2H, *J* = 6.6 Hz, CH_2CH$_2$NCO), 2.51-2.45 (m, 5H, 2×CH_2N, C*H*CO), 2.12 (s, 3H, CH_3-Py), 2.04-2.00 (m, 2H, CH_2), 1.81-1.71 (m, 4H, 2×CH_2), 1.59-1.46 (m, 6H, 3×CH_2).

*4.1.3.9. N-(1-(4-fluorobenzyl)-4-methyl-2-oxo-1,2-dihydropyridin-3-yl)-4-methylcyclohexyl carboxamide (**30**).*

Purification by flash column chromatography (1:1 hexane-ethyl acetate). Yellow oil (0.706 g, 1.98 mmol, Yield: 40 %). ^{1}H-NMR ($CDCl_3$) δ for isomeric mixture (about 1:1): 7.80 (bs, 2H, 2×NH), 7.24, 6.98 (AA'XX' system, 4H, Ar-*H*), 7.04, 7.39 (2d, each 1H, *J* = 7.0 Hz, H_6-Py), 6.11, 6.10 (2d, each 1H, *J* = 7.0 Hz, H_5-Py), 5.05, 5.04 (2s, each 2H, PhCH_2N), 2.51, 2.27 (2m, each 1H, C*H*CO), 2.11, 2.09 (2s, each 3H, CH_3-Py), 2.09-1.95 (m, 2H, CH_2), 1.78-1.63 (m, 3H, CH, CH$_2$), 1.59-1.24 (m, 4H, CH_2), 0.93, 0.88 (2d, each 3H, *J* = 6.8 Hz, CH_3).

*4.1.3.10. N-(4-methyl-2-oxo-1,2-dihydropyridin-3-yl)-cycloheptane-carboxamide (**34**).*

Triturated with CH_3OH. White solid (0.643 g, 2.59 mmol, Yield: 55 %). ^{1}H-NMR ($CDCl_3$) δ: 7.71 (bs, 1H, NH), 7.07 (d, 1H, *J* = 6.8 Hz, H_6-Py), 6.19 (d, 1H, *J* = 6.8 Hz, H_5-Py), 2.53-2.48 (m, 1H,

C*H*CO), 2.16 (s, 3H, C*H*$_3$-Py), 2.15-1.99 (m, 2H, C*H*$_2$), 1.80-1.75 (m, 4H, 2×C*H*$_2$), 1.59-1.42 (m, 6H, 3×C*H*$_2$).

*4.1.4. General procedure for the synthesis of compounds **27-29.***

The suitable anhydride (1.32 mmol) was added to a solution of compound **10** (0.255 g, 1.01 mmol) in toluene (2.75 mL) and the reaction mixture, was stirred for 16 h at 110 °C. The solvent was evaporated under reduced pressure. The residue obtained was dissolved in $CHCl_3$ and washed three times with water. The organic phase was then dried over Na_2SO_4, filtered and concentrated in vacuum.

*4.1.4.1. N-(1-(4-fluorobenzyl)-4-methyl-2-oxo-1,2-dihydropyridin-3-yl)-acetamide (**27**).*

Purification by flash column chromatography (ethyl acetate + 1% CH_3COOH). Ocher oil (0.064 g, 0.232 mmol, Yield: 23 %). ^{1}H-NMR ($CDCl_3$) δ: 7.51 (bs, 1H, NH), 7.29, 7.02 (AA'XX' system, 4H, Ar-*H*), 7.07 (d, 1H, *J* = 7.2 Hz, *H*$_6$-Py), 6.12 (d, 1H, *J* = 7.2 Hz, *H*$_5$-Py), 5.08 (s, 2H, PhC*H*$_2$N), 2.20 (s, 3H, C*H*$_3$-Py), 2.18 (s, 3H, C*H*$_3$CO).

*4.1.4.2. N-(1-(4-fluorobenzyl)-4-methyl-2-oxo-1,2-dihydropyridin-3-yl)-benzamide (**28**).*

Purification by flash column chromatography (1:1 hexane-ethyl acetate). Yellow solid (0.078 g, 0.232 mmol, Yield: 23 %). ^{1}H-NMR ($CDCl_3$) δ: 8.32 (bs, 1H, NH), 7.94-7.91 (m, 2H, Ar-*H*), 7.55-7.51 (m, 1H, Ar-*H*), 7.43, 6.99 (AA'XX' system, 4H, Ar-*H*), 7.26 (m, 2H, Ar-*H*), 7.09 (d, 1H, *J* = 7.2 Hz, *H*$_6$-Py), 6.16 (d, 1H, *J* = 7.2 Hz, *H*$_5$-Py), 5.08 (s, 2H, PhC*H*$_2$N), 2.22 (s, 3H, C*H*$_3$-Py).

*4.1.4.3. N-(1-(4-fluorobenzyl)-4-methyl-2-oxo-1,2- dihydropyridin-3-yl)-heptanamide (**29**).*

Ocher oil (0.115 g, 0.334 mmol, Yield: 33 %). ^{1}H-NMR ($CDCl_3$) δ: 7.69 (bs, 1H, NH), 7.26, 7.02 (AA'XX' system, 4H, Ar-*H*), 7.06 (d, 1H, *J* = 6.8 Hz, *H*$_6$-Py), 6.12 (d, 1H, *J* = 6.8 Hz, *H*$_5$-Py), 5.07

(s, 2H, PhCH_2N), 2.46-2.40 (m, 2H, CH_2CO), 2.14 (s, 3H, CH_3-Py), 1.70-1.59 (m, 2H, CH_2CH$_2$CO), 1.38-1.25 (m, 6H, 3×CH_2), 0.87 (t, 3H, J = 7.4 Hz, CH_3).

*4.1.5. Cycloheptyl (1-(4-fluorobenzyl)-4-methyl-2-oxo-1,2-dihydropyridin-3-yl)carbamate (**31**).*

Compound **10** (0.357 mg, 1.54 mmol) was added dropwise to a solution of triethylamine (0.539 mL, 3.99 mmol) and cycloheptylchloroformate (0.705 g, 3.99 mmol) (previously prepared with a reaction between BTC (Bis(trichloromethyl) carbonate) and cycloheptanol) in anhydrous dichloromethane (12 mL). The reaction mixture was stirred at room temperature for 4 h. After that, the resulting solution was washed three times with water, dried over Na_2SO_4, filtered and evaporated under reduced pressure. The brown oil obtained was purified by flash chromatography on silica gel (3:7 hexane-ethyl acetate) and subsequently washed with hexane to afford compound **31**. Brown oil (0.042 g, 0.113 mmol, Yield: 7 %). ^{1}H-NMR ($CDCl_3$) δ: 7.29-7.26 (m, 2H, Ar-*H*), 7.04-7.00 (m, 3H, Ar-*H*, H_6-Py), 6.78 (bs, 1H, NH), 6.09 (d, 1H, J = 6.8 Hz, H_5-Py), 5.07 (s, 2H, PhCH_2N), 4.85-4.83 (m, 1H, C*H*O), 2.18 (s, 3H, CH_3-Py), 1.98-1.93 (m, 2H, CH_2), 1.74-1.46 (m, 10H, 5×CH_2).

*4.1.6. 1-cycloheptyl-3-(1-(4-fluorobenzyl)-4-methyl-2-oxo-1,2-dihydropyridin-3-yl)-urea (**32**).*

Cycloheptylisocyanate (0.103 mL, 0.780 mmol) was added dropwise to a solution of compound **10** (0.181 g, 0.780 mmol) in dry $CHCl_3$ and the reaction mixture was stirred at room temperature for 48 h. The solution obtained was evaporated under reduced pressure and the crude product obtained triturated with diethyl ether to afford compound **32**. White solid (0.199 g, 0.536 mmol, Yield: 68 %). ^{1}H-NMR ($CDCl_3$) δ: 7.28-7.25 (m, 4H, Ar-*H,* 2×NH), 7.04-7.00 (m, 3H, Ar-*H, H*$_6$-Py), 6.17 (d, 1H, J = 6.4 Hz, H_5-Py), 5.10 (s, 2H, PhCH_2N), 3.84-3.80 (m, 1H, C*H*N), 2.24 (s, 3H, CH_3-Py), 1.99-1.84 (m, 2H, CH_2), 1.65-1.36 (m, 10H, 5×CH_2).

*4.1.7. General procedure for the synthesis of compounds **A1-A8**, **B1-B6**, **35** and **36.***

A solution of Br_2 (0.13 mL, 2.52 mmol) in $CHCl_3$ (1.68 mL) was added dropwise to a solution of derivatives **19-32** (1.01 mmol) in $CHCl_3$. Reaction mixture was stirred at room temperature for 12 h. The solution obtained was washed three times with a saturated aqueous solution of $Na_2S_2O_3$. The organic phase was dried over Na_2SO_4, filtered and evaporated under reduced pressure.

*4.1.7.1. N-(5-bromo-1-(2-fluorobenzyl)-4-methyl-2-oxo-1,2-dihydropyridin-3yl)–cycloheptane-carboxamide (**A1**) (SV-10a).*

Purification by flash column chromatography (3:7 petroleum ether-ethyl acetate). Brown solid (0.180 g, 0.414 mmol, Yield: 41 %). Mp: 148-150 °C. ^{1}H-NMR ($CDCl_3$) δ: 7.55 (bs, 1H, NH), 7.46 (s, 1H, *H*$_6$-Py), 7.41 (m, 1H, Ar-*H*), 7.32 (m, 1H, Ar-*H*), 7.11-7.05 (m, 2H, Ar-*H*), 5.12 (s, 2H, PhC*H*$_2$N), 2.52-2.43 (m, 1H, C*H*CO), 2.14 (s, 3H, C*H*$_3$-Py), 2.02-1.98 (m, 2H, C*H*$_2$), 1.80-1.69 (m, 4H, 2×C*H*$_2$), 1.58-1.47 (m, 6H, 3×C*H*$_2$). ^{13}C-NMR ($CDCl_3$) δ: 176.02 (*C*=O), 161.08 (d, $J_{C\text{-}F}$= 245 Hz, Ar-*C*F), 158.50 (*C*$_2$-Py), 142.17 (*C*$_3$-Py),132.71 (*C*$_4$-Py),131.41 (d, $J_{C,F}$= 3 Hz, Ar-*C*H), 130.51 (d, $J_{C,F}$ = 8 Hz, Ar-*C*H), 126.43 (*C*$_6$-Py),124.71 (d, $J_{C,F}$ = 3 Hz, Ar-*C*H), 122.44 (d, $J_{C,F}$ = 14 Hz, Ar-*C*), 115.73 (d, $J_{C,F}$= 22 Hz, Ar-*C*H), 103.82 (*C*$_5$-Py), 47.85, (Ph*C*H$_2$N), 46.80 (*C*HCO), 31.77, 28.20, 26.68, (6×*C*H$_2$), 20.57 (*C*H$_3$-Py). HPLC analysis: retention time = 16.32 min; peak area 96.21 % (280 nm). HRMS-ESI: m /z calcd for $C_{21}H_{24}BrFN_2O_2$ $[M+H]^+$, 435.10780; found 435.10730.

*4.1.7.2. N-(5-bromo-1-(3-fluorobenzyl)-4-methyl-2-oxo-1,2-dihydropyridin-3yl)-cycloheptane-carboxamide (**A2**).*

Purification by flash column chromatography (7:3 ethyl acetate-petroleum ether). Brown solid (0.435 g, 1.00 mmol, Yield: 99 %). Mp: 138-140 °C. ^{1}H-NMR ($CDCl_3$) δ: 7.48 (bs, 1H, NH), 7.34 (s, 1H, *H*$_6$-Py), 7.33-7.30 (m, 1H, Ar-*H*), 7.06-6.98 (m, 3H, Ar-*H*), 5.08 (s, 2H, PhC*H*$_2$N), 2.54-2.48 (m, 1H, C*H*CO), 2.17 (s, 3H, C*H*$_3$-Py), 2.08-2.00 (m, 2H, C*H*$_2$), 1.82-1.72 (m, 4H, 2×C*H*$_2$), 1.60-1.40 (m, 6H, 3×C*H*$_2$). ^{13}C-NMR ($CDCl_3$) δ: 176.11 (C=O), 163.00 (d, $J_{C\text{-}F}$= 246 Hz, Ar-*C*F), 158.38 (C$_2$-Py), 142.58 (C$_3$-Py), 137.85 (d, $J_{C,F}$= 7 Hz, Ar-*C*), 132.29 (C$_4$-Py), 130.65 (d, $J_{C,F}$= 8 Hz, Ar-*C*H), 126.58

(C_6-Py), 123.65 (d, $J_{C,F}$= 3 Hz, Ar-*C*H), 115.42 (d, $J_{C,F}$= 20 Hz, Ar-*C*H), 115.11 (d, $J_{C,F}$= 22 Hz, Ar-*C*H), 104.15 (C_5-Py), 52.13 (PhCH_2N), 47.68 (*C*HCO), 31.70, 28.15, 26.61 (6×CH_2), 20.53 (*C*H_3-Py). HPLC analysis: retention time = 15.77 min; peak area 96.67 % (280 nm). HRMS-ESI: m /z calcd for $C_{21}H_{24}BrFN_2O_2$ $[M+H]^+$, 435.10780; found 435.10745.

*4.1.7.3. N-(5-bromo-1-benzyl-4-methyl-2-oxo-1,2-dihydropyridin-3yl)-cycloheptane-carboxamide (**A3**).*

Purification by flash column chromatography (3:7 petroleum ether- ethyl acetate). Brown solid (0.139 g, 0.334 mmol, Yield: 33 %). Mp: 183-185 °C. ^{1}H-NMR ($CDCl_3$) δ: 7.49 (bs, 1H, NH), 7.36-7.34 (m, 4H, Ar-*H, H*$_6$-Py), 7.29-7.27 (m, 2H, Ar-*H*), 5.10 (s, 2H, PhCH_2N), 2.53-2.48 (m, 1H, C*H*CO), 2.16 (s, 3H, CH_3-Py), 2.06-2.01 (m, 2H, CH_2), 1.82-1.72 (m, 4H, 2×CH_2), 1.59-1.43 (m, 6H, 3×CH_2). ^{13}C-NMR ($CDCl_3$) δ: 176.09 (*C*=O), 158.59 (C_2-Py), 141.96 (C_3-Py), 135.49 (Ar-*C*), 132.29 (C_4-Py), 129.16, 128.53, 128.31 (Ar-*C*H), 126.60 (C_6-Py), 103.95 (C_5-Py), 52.60 (Ph*C*H_2N), 47.94 (*C*HCO), 31.82, 28.24, 26.71(6×*C*H_2), 20.63 (*C*H_3-Py). HPLC analysis: retention time = 15.73 min; peak area 99.00 % (280 nm). HRMS-ESI: m /z calcd for $C_{21}H_{24}BrFN_2O_2$ $[M+H]^+$, 435,10780; found 435,10745. HRMS-ESI: m /z calcd for $C_{21}H_{25}BrN_2O_2$ $[M+H]^+$, 417.11722; found 417.11661.

*4.1.7.4. N-(5-bromo-1-(4-chlorobenzyl)-4-methyl-2-oxo-1,2-dihydropyridin-3yl)-cycloheptane-carboxamide (**A4**).*

Purification by flash column chromatography (1:1 petroleum ether-ethyl acetate). Brown solid (0.082 g, 0.182 mmol, Yield: 18 %). Mp: > 200 °C. ^{1}H-NMR ($CDCl_3$) δ: 7.47 (bs, 1H, NH), 7.34-7-32 (m, 3H, Ar-*H, H*$_6$-Py), 7.24-7.22 (m, 2H, Ar-*H*), 5.05 (s, 2H, PhCH_2N), 2.53-2.47 (m, 1H, C*H*CO), 2.16 (s, 3H, CH_3-Py), 2.04-1.99 (m, 2H, CH_2), 1.83-1.72 (m, 4H, 2×CH_2), 1.54-1.46 (m, 6H, 3×CH_2). ^{13}C-NMR ($CDCl_3$) δ: 176.05 (*C*=O), 158.43 (C_2-Py), 142.18 (C_3-Py), 134.52, 134.02 (2×Ar-*C*), 132.10 (C_4-Py), 129.64, 129.32 (Ar-*C*H), 126.66 (C_6-Py), 104.13 (C_5-Py), 52.10 (Ph*C*H_2N), 47.92 (*C*HCO), 31.81, 28.23, 26.70 (6×*C*H_2), 20.64 (*C*H_3-Py). HPLC analysis: retention time = 15.73 min;

peak area 95.40 % (280 nm). HRMS-ESI: m /z calcd for $C_{21}H_{24}BrClN_2O_2$ $[M+H]^+$, 451.07825; found 451.07870.

*4.1.7.5. N-(5-bromo-1-(2-chlorobenzyl)-4-methyl-2-oxo-1,2-dihydropyridin-3yl)-cycloheptane-carboxamide (**A5**) (SB-13a).*

Purification by flash column chromatography (6:4 petroleum ether-ethyl acetate). Beige solid (0.246 g, 0.545 mmol, Yield: 54 %). Mp: 166-168 °C. ^{1}H-NMR ($CDCl_3$) δ: 7.49 (bs, 1H, N*H*), 7.42-7.40 (m, 2H, Ar-*H, H*$_6$-Py), 7.30-7.22 (m, 3H, Ar-*H*), 5.22 (s, 2H, PhC*H*$_2$N), 2.52-2.48 (m, 1H, C*H*CO), 2.17 (s, 3H, C*H*$_3$-Py), 2.06-1.99 (m, 2H, C*H*$_2$), 1.83-1.71 (m, 4H, 2×C*H*$_2$),1.62-1.47 (m, 6H, 3×C*H*$_2$). ^{13}C-NMR ($CDCl_3$) δ: 176.20 (*C*=O), 158.75 (*C*$_2$-Py), 142.40 (*C*$_3$-Py), 133.79, 133.01 (2×Ar-*C*), 132.72 (*C*$_4$-Py), 130.53, 130.10, 129.99, 127.68 (Ar-*C*H), 126.64 (*C*$_6$-Py), 104.11 (*C*$_5$-Py), 50.30 (Ph*C*H$_2$N), 48.07 (*C*HCO), 31.93, 28.36, 26.83 (6×*C*H$_2$), 20.80 (*C*H$_3$-Py). HPLC analysis: retention time = 20.18 min; peak area 95.60 % (280 nm). HRMS-ESI: m /z calcd for $C_{21}H_{24}BrClN_2O_2$ $[M+H]^+$, 451.07825; found 451.07745.

*4.1.7.6. N-(5-bromo-1-(4-iodobenzyl)-4-methyl-2-oxo-1,2-dihydropyridin-3yl)-cycloheptane-carboxamide (**A6**).*

Purification by flash column chromatography (1:1 petroleum ether-ethyl acetate). Brown solid (0.099 g, 0.182 mmol, Yield: 18 %). Mp: > 200 °C. ^{1}H-NMR ($CDCl_3$) δ: 7.68, 7.03 (AA'XX' system, 4H,Ar-*H*), 7.47 (bs, 1H, NH), 7.32 (s, 1H, *H*$_6$-Py), 5.02 (s, 2H, PhC*H*$_2$N), 2.52-2.46 (m, 1H, C*H*CO), 2.16 (s, 3H, C*H*$_3$-Py), 2.03-2.00 (m, 2H, C*H*$_2$), 1.82-1.71 (m, 4H, 2×C*H*$_2$), 1.57-1.44 (m, 6H, 3×C*H*$_2$). ^{13}C-NMR ($CDCl_3$) δ: 176.05 (*C*=O), 158.46 (*C*$_2$-Py), 142.12 (*C*$_3$-Py), 138.27 (Ar-*C*H), 135.20 (Ar-*C*), 132.07 (*C*$_4$-Py), 130.13 (Ar-*C*H,C$_6$-Py), 104.19 (*C*$_5$-Py), 94.27 (Ar-*C*I), 52.29 (Ph*C*H$_2$N), 47.99 (*C*HCO), 31.83, 28.25, 26.72 (6×*C*H$_2$), 20.69 (*C*H$_3$-Py). HPLC analysis: retention time = 11.90 min; peak area 96.00 % (280 nm). HRMS-ESI: m /z calcd for $C_{21}H_{24}BrIN_2O_2$ $[M+H]^+$, 543.01386; found 543.01361.

*4.1.7.7. N-(5-bromo-1-(4-bromobenzyl)-4-methyl-2-oxo-1,2-dihydropyridin-3yl)-cycloheptane-carboxamide (**A7**).*

Purification by flash column chromatography (6:4 hexane-ethyl acetate). Brown solid (0.426 g, 0.859 mmol, Yield: 85 %). Mp: 180-182 °C. ^{1}H-NMR ($CDCl_3$) δ: 7.48, 7.17 (AA'XX' system, 4H, Ar-*H*), 7.32 (s, 1H, *H*$_6$-Py), 5.04 (s, 2H, PhC*H*$_2$N), 2.52-2.48 (m, 1H, C*H*CO), 2.16 (s, 3H, C*H*$_3$-Py), 2.04-1.99 (m, 2H, C*H*$_2$), 1.81-1.71 (m, 4H, 2×C*H*$_2$), 1.59-1.42 (m, 6H, 3×C*H*$_2$). ^{13}C-NMR ($CDCl_3$) δ: 175.99 (*C*=O), 158.34 (*C*$_2$-Py), 142.25 (*C*$_3$-Py), 134.37 (Ar-*C*), 132.19 (Ar-*C*H), 132.00 (*C*$_4$-Py), 129.84 (Ar-*C*H), 126.54 (*C*$_6$-Py), 122.55 (Ar-*C*), 104.15 (*C*$_5$-Py), 52.10 (Ph*C*H$_2$N), 47.81 (*C*HCO), 31.70, 28.12, 26.59(6×*C*H$_2$), 20.55 (*C*H$_3$-Py). HPLC analysis: retention time = 11.48 min; peak area 95.00 % (280 nm). HRMS-ESI: m /z calcd for $C_{21}H_{24}Br_2N_2O_2$ $[M+H]^+$, 495.02773; found 495.02725.

*4.1.7.8. N-(5-bromo-1-(2-morpholinoethyl)-4-methyl-2-oxo-1,2-dihydropyridin-3-yl)-cycloheptane-carboxamide (**A8**).*

Purification by flash column chromatography (9.5:0.5 ethyl acetate-methanol). Beige solid (0.111 g, 0.253 mmol, Yield: 25 %). Mp: 130-133 °C. ^{1}H-NMR ($CDCl_3$) δ:) 7.52 (bs, 1H, NH), 7.39 (s, 1H, *H*$_6$-Py), 4.00 (t, 2H, *J* = 6.2 Hz. C*H*$_2$NCO), 3.69-3.67 (m, 4H, 2×C*H*$_2$O), 2.63 (t, 2H, *J* = 6.2 Hz, C*H*$_2$CH$_2$NCO), 2.50-2.48 (m, 5H, 2×C*H*$_2$N, C*H*CO), 2.15 (s, 3H, C*H*$_3$-Py), 2.01-1.98 (m, 2H, C*H*$_2$), 1.51-1.70 (m, 4H, 2×C*H*$_2$),), 1.58-1.41 (m, 6H, 3×C*H*$_2$).^{13}C-NMR ($CDCl_3$) δ: 176.09 (*C*=O), 158.31 (*C*$_2$-Py), 142.28 (*C*$_3$-Py), 133.50 (*C*$_4$-Py), 126.12 (*C*$_6$-Py), 103.09 (*C*$_5$-Py), 66.96 (2×*C*H$_2$O), 56.93 (*C*H$_2$NCO), 53.68 (2×*C*H$_2$N), 47.77 (*C*HCO), 46.58 *C*H$_2$CH$_2$NCO), 31.76, 28.20, 26.66 (6×*C*H$_2$), 20.46 (*C*H$_3$-Py). HPLC analysis: retention time = 15.69 min; peak area 95.50 % (280 nm). HRMS-ESI: m /z calcd for $C_{20}H_{30}BrN_3O_3$ $[M+H]^+$, 440.15433; found 440.15421.

*4.1.7.9. N-(5-bromo-1-(4-fluorobenzyl)-4-methyl-2-oxo-1,2-dihydropyridin-3-yl)-acetamide (**B1**).*

Purification by flash column chromatography (ethyl acetate + 2% CH_3OH). Brown oil (0.050 g, 0.141 mmol, Yield: 14 %). ^{1}H-NMR ($CDCl_3$) δ: 7.59 (bs, 1H, NH), 7.36 (s, 1H, *H*$_6$-Py), 7.28, 7.04 (AA'XX' system, 4H, Ar-*H*), 5.06 (s, 2H, PhC*H*$_2$N), 2.21 (s, 3H, C*H*$_3$-Py), 2.19 (s, 3H, C*H*$_3$CO). ^{13}C-NMR ($CDCl_3$) δ: 169.22 (*C*=O), 162.85 (d, J_{C-F}= 246 Hz, Ar-*C*F), 158.46 (C_2-Py), 143.87 (*C*$_3$-Py), 131.49 (*C*$_4$-Py), 131.10 (d, J_{C-F}= 3 Hz, Ar-*C*), 130.28 (d, J_{C-F}= 8 Hz, 2×Ar-*C*H), 126.50 (*C*$_6$-Py), 116.19 (d, J_{C-F}= 22 Hz, 2×Ar-*C*H), 104.52 (C_5-Py), 52.36 (Ph*C*H$_2$N), 23.85 (*C*H$_3$CO), 20.74 (*C*H$_3$-Py). HPLC analysis: retention time = 16.23 min; peak area 96.40 % (280 nm). HRMS-ESI: m /z calcd for $C_{15}H_{14}BrFN_2O_2$ $[M+H]^+$, 353.02955; found 353.02921.

*4.1.7.10. N-(5-bromo-1-(4-fluorobenzyl)-4-methyl-2-oxo-1,2-dihydropyridin-3-yl)-benzamide (**B2**).*

Yellow solid (0.214 g, 0.515 mmol, 51 %). Mp: 153-156 °C. ^{1}H-NMR ($CDCl_3$) δ: 8.27 (bs, 1H, NH), 7.94-7.92 (m, 2H, Ar-*H*), 7.57-7.55 (m, 1H, Ar-*H*), 7.48, 7.05 (AA'XX' system, 4H, Ar-*H*), 7.40 (s, 1H, *H*$_6$-Py), 7.32-7.29 (m, 2H, Ar-*H*), 5.09 (s, 2H, PhC*H*$_2$N), 2.28 (s, 3H, C*H*$_3$-Py). ^{13}C-NMR ($CDCl_3$) δ: 166.05 (*C*=O), 162.82 (d, J_{C-F}= 246 Hz, Ar-*C*F), 158.49 (*C*$_2$-Py), 142.72 (*C*$_3$-Py), 133.83 (Ar-*C*), 132.43 (d, J_{C-F}= 4 Hz, Ar-*C*), 131.18 (*C*$_4$-Py), 130.26 (d, J_{C-F}= 8 Hz, 2×Ar-*C*H), 128.83, 127.85, 127.59, 127.33 (Ar-*C*H), 126.88 (*C*$_6$-Py), 116.16 (d, J_{C-F}= 22 Hz, 2×Ar-*C*H), 104.42 (*C*$_5$-Py), 52.27 (Ph*C*H$_2$N), 20.97 (*C*H$_3$-Py). HPLC analysis: retention time = 15.94 min; peak area 95.77 % (280 nm). HRMS-ESI: m /z calcd for $C_{20}H_{16}BrFN_2O_2$ $[M+H]^+$, 415.04520; found 415.04483.

*4.1.7.11. N-(5-bromo-1-(4-fluorobenzyl)-4-methyl-2-oxo-1,2-dihydropyridin-3-yl) heptanamide (**B3**).*

Purification by flash column chromatography (6:4 hexane-ethyl acetate). Ocher oil (0.077 g, 0.182 mmol, 18 %). ^{1}H-NMR ($CDCl_3$) δ: 7.68 (bs, 1H, NH), 7.35 (s, 1H, *H*$_6$-Py), 7.27, 7.03 (AA'XX' system, 4H, Ar-*H*), 5.05 (s, 2H, PhC*H*$_2$N), 2.41 (t, 2H, *J* = 7.6 Hz, C*H*$_2$CO), 2.17 (s, 3H, C*H*$_3$-Py), 1.74-1.66 (m, 2H, C*H*$_2$CH$_2$CO), 1.37-1.24 (m, 6H, 3×C*H*$_2$), 0.87 (t, 3H, *J* = 6.4 Hz, C*H*$_3$). ^{13}C-NMR

($CDCl_3$) δ: 172.11 (*C*=O), 162.79 (d, $J_{C\text{-}F}$= 246 Hz, Ar-*C*F), 158.43 (*C*$_2$-Py), 142.63 (*C*$_3$-Py), 132.34 (*C*$_4$-Py), 131.29 (d, $J_{C\text{-}F}$= 4 Hz, Ar-*C*), 130.22 (d, $J_{C\text{-}F}$= 9 Hz, 2×Ar-*C*H), 126.58 (*C*$_6$-Py), 116.11 (d, $J_{C\text{-}F}$= 21 Hz, 2×Ar-*C*H), 104.14 (*C*$_5$-Py), 52.11 (Ph*C*H$_2$N), 37.22 (*C*H$_2$CO), 31.61, 29.04, 25.76, 22.60 (4×*C*H$_2$), 20.78 (*C*H$_3$-Py), 14.14 (*C*H$_3$). HPLC analysis: retention time = 13.40 min; peak area 96.00 % (280 nm). HRMS-ESI: m /z calcd for $C_{20}H_{24}BrFN_2O_2$ $[M+H]^+$, 423.10780; found 423.10718.

*4.1.7.12. N-(5-bromo-1-(4-fluorobenzyl)-4-methyl-2-oxo-1,2-dihydropyridin-3-yl)-4-methylcyclohexyl carboxamide (**B4**).*

Purification by flash column chromatography (6:4 hexane-ethyl acetate). Brown oil (0.215 g, 0.495 mmol, Yield: 49 %). ^{1}H-NMR ($CDCl_3$) δ for isomeric mixture (about 1:1): 7.62, 7.54 (2bs, each 1H, NH), 7.34, 7.33 (2s, each 1H, *H*$_6$-Py), 7.28, 7.04 (AA'XX' system, 4H, Ar-*H*), 5.06, 5.05 (2s, each 2H, PhC*H*$_2$N), 2.87, 2.53 (2m, each 1H, C*H*CO), 2.17, 2.15 (2s, each 3H, C*H*$_3$-Py); 2.03-1.95 (m, 2H, C*H*$_2$), 1.82-1.67 (m, 3H, CH, CH$_2$), 1.63-1.51 (m, 2H, C*H*$_2$), 1.45-1.37 (m, 2H, C*H*$_2$), 0.95, 0.90 (2d, each 3H, *J* = 6.6 Hz, C*H*$_3$). ^{13}C-NMR ($CDCl_3$) δ for isomeric mixture (about 1:1): 175.22, 174.65 (2×*C*=O), 162.74 (d, $J_{C\text{-}F}$= 246 Hz, Ar-*C*F), 158.40, 158.38 (2×*C*$_2$-Py), 142.71, 142.55 (2×*C*$_3$-Py), 132.27 (d, $J_{C\text{-}F}$= 11 Hz, Ar-*C*H), 131.26 (d, $J_{C\text{-}F}$= 3 Hz, Ar-*C*), 126.69, 126.56 (2×*C*$_6$-Py), 116.05 (d, $J_{C\text{-}F}$= 21 Hz, Ar-*C*H) 104.24 (C$_5$-Py), 52.11, 52.06 (2×Ph*C*H$_2$N), 45.75, 43.12 (2×*C*HCO), 34.40, 32.04, 31.28, 29.78 (4×*C*H$_2$), 26.13 (*C*HCH$_3$), 22.53 (*C*H$_3$), 20.71, 20.60 (2×*C*H$_3$-Py). HPLC analysis: retention time = 14.56 min; peak area 97.00 % (280 nm). HRMS-ESI: m /z calcd for $C_{21}H_{24}BrFN_2O_2$ $[M+H]^+$, 435.10780; found 435.10754.

*4.1.7.13. Cycloheptyl-(5-bromo-1-(4-fluorobenzyl)-4-methyl-2-oxo-1,2-dihydropyridin-3-yl)-carbamate (**B5**).*

Purification by flash column chromatography (7:3 ethyl acetate-hexane). Ocher oil (0.141 g, 0.313 mmol, Yield: 31 %). ^{1}H-NMR ($CDCl_3$) δ: 7.31 (s, 1H, *H*$_6$-Py), 7.29, 7.03 (AA'XX' system, 4H, Ar-*H*), 6.86 (bs, 1H, NH), 5.06 (s, 2H, PhC*H*$_2$N), 4.87-4.83 (m, 1H, C*H*O), 2.23 (s, 3H, C*H*$_3$-Py), 1.99-

1.92 (m, 2H, CH_2), 1.72-1.64 (m, 4H, 2×CH_2), 1.57-1.54 (m, 6H, 3×CH_2). ^{13}C-NMR ($CDCl_3$) δ: 161.58 (Ar-*C*F), 158.48 (*C*$_2$-Py), 153.98 (*C*ONH), 142.34 (*C*$_3$-Py), 131.92 (d, J_{C-F}= 8 Hz, Ar-*C*), 131.38 (*C*$_4$-Py), 130.29 (d, J_{C-F}= 8 Hz, 2×Ar-*C*H), 127.18 (*C*$_6$-Py), 116.12 (d, J_{C-F}= 22 Hz, 2×Ar-*C*H), 104.02 (*C*$_5$-Py), 52.07 (Ph*C*H$_2$N), 34.06 (*C*HO), 29.82, 28.40, 22.91 (4×*C*H$_2$), 20.34 (*C*H$_3$-Py). HPLC analysis: retention time = 15.48 min; peak area 95.30 % (280 nm). HRMS-ESI: m /z calcd for $C_{21}H_{24}BrFN_2O_3$ $[M+H]^+$, 451.10271; found 451.10236.

4.1.7.14. 1-(5-bromo-1-(4-fluorobenzyl)-4-methyl-2-oxo-1,2-dihydropyridin-3-yl)-3-cycloheptyl-urea (**B6**).

Yellow solid (0.273 g, 0.606 mmol, Yield: 60 %). Mp: > 200 °C. ^{1}H-NMR ($CDCl_3$) δ: 7.29 (s, 1H, *H*$_6$-Py); 7.28,7.04 (AA'XX' system, 4H, Ar-*H*), 5.31 (bs, 1H, NH), 5.08 (s, 2H, PhC*H*$_2$N); 3.76-3.73 (m, 1H, C*H*N), 2.27 (s, 3H, C*H*$_3$-Py), 1.96-1.92 (m, 2H, C*H*$_2$), 1.59-1.57 (m, 4H, 2×C*H*$_2$), 1.48-1.40 (m, 6H, 3×C*H*$_2$). ^{13}C-NMR ($CDCl_3$) δ: 162.78 (d, J_{C-F}= 247 Hz, Ar-*C*F), 159.12 (*C*$_2$-Py), 154.94 (*C*ONH), 142.10 (*C*$_3$-Py), 131.25 (d, J_{C-F}= 4 Hz, Ar-*C*), 130.98 (*C*$_4$-Py), 130.14 (d, J_{C-F}= 8 Hz, 2×Ar-*C*H), 128.52 (*C*$_6$-Py), 116.12 (d, J_{C-F}= 21 Hz, 2×Ar-*C*H), 105.17 (*C*$_5$-Py), 52.09 (Ph*C*H$_2$N), 51.67 (*C*HN), 35.56 (*C*HO), 28.06, 24.19 (4×*C*H$_2$), 20.63 (*C*H$_3$-Py). HPLC analysis: retention time = 16.52 min; peak area 96.84 % (280 nm). HRMS-ESI: m /z calcd for $C_{21}H_{25}BrFN_3O_2$ $[M+H]^+$, 450.11869; found 450.11795.

*4.1.7.15. N-(5-bromo-4-methyl-2-oxo-1,2-dihydropyridin-3-yl)-cycloheptane-carboxamide (**35**).*

Purification by flash column chromatography (ethyl acetate). Yellow solid (0.126 g, 0.384 mmol, Yield: 38 %). ^{1}H-NMR ($CDCl_3$) δ: 7.44 (bs, 1H, NH), 7.39 (s, 1H, *H*$_6$-Py), 2.54-2.50 (m, 1H, C*H*CO), 2.20 (s, 3H, C*H*$_3$-Py), 2.04-2.01 (m, 2H, C*H*$_2$), 1.79-1.73 (m, 4H, 2×C*H*$_2$), 1.59-1.49 (m, 6H, 3×C*H*$_2$).

*4.1.7.16. 2-hydroxy-5-bromo-4-methyl-3-nitropyridine (**36**).*

Yellow solid (0.351 g, 1.51 mmol, Yield: 77 %). ^{1}H-NMR ($CDCl_3$) δ: 7.69 (s, 1H, H_6-Py), 2.36 (s, 3H, CH_3-Py).

*4.1.8. General procedure for the synthesis of compounds **A9**, **A10**, **B7***

CsF (83.5 mg, 0.55 mmol) was added to a solution of compound **35** or **36** (0.180 mmol) in anhydrous DMF (0.55 mL). Reaction mixture was stirred at room temperature for 1 h. Then the appropriate alkyl chloride (0.55 mmol) was added dropwise and the reaction was stirred at 50 °C for 12 h. DMF was removed under reduced pressure. The residue obtained was dissolved in $CHCl_3$ and washed 3 times with water. The organic phase was dried over Na_2SO_4 filtered and evaporated under reduced pressure.

*4.1.8.1. N-(5-bromo-4-methyl-2-oxo-1-pentyl-1,2-dihydropyridin-3-yl)-cycloheptane-carboxamide (**A9**).*

Purification by flash column chromatography (8:2 hexane-ethyl acetate). Brown solid (0.022 g, 0.056 mmol, Yield: 31 %) Mp: 118-121 °C. ^{1}H-NMR ($CDCl_3$) δ: 7.53 (bs, 1H, NH), 7.32 (s, 1H, H_6-Py), 3.88 (t, 2H, J = 7.6 Hz, CH_2N), 2.53-2.48 (m, 1H, C*H*CO),), 2.15 (s, 3H, CH_3-Py), 2.04-1.99 (m, 2H, CH_2), 1.80-1.69 (m, 6H, 3×CH_2), 1.58-1.41 (m, 6H, 3×CH_2), 1.37.1.21 (m, 4H, 2×CH_2), 0.90 (t, 3H, J = 7.2 Hz, CH_3). ^{13}C-NMR ($CDCl_3$) δ: 176.14 (*C*=O), 170.48(C_2-Py), 141.79 (C_3-Py), 132.67 (C_4-Py), 126.44 (C_6-Py), 103.50 (C_5-Py), 50.30 (*C*H_2N), 47.85 (*C*HCO), 31.79, 29.03, 28.79, 28.23, 26.69, 22.36 (9×*C*H_2), 20.53 (*C*H_3-Py), 13.99 (*C*H_3). HPLC analysis: retention time = 13.07 min; peak area 95.00 % (280 nm). HRMS-ESI: m /z calcd for $C_{19}H_{29}BrN_2O_2$ $[M+H]^+$, 397.14852; found 397.14819.

*4.1.8.2. N-(5-bromo-4-methyl-2-oxo-1-hydroxypentyl-1,2-dihydropyridin-3-yl)-cycloheptane-carboxamide (**A10**).*

Purification by flash column chromatography (1:9 hexane-ethyl acetate). White solid (0.022 g, 0.052 mmol, Yield: 29 %). Mp: 193-195 °C. ^{1}H-NMR (MeOD) δ: 7.88 (s, 1H, NH), 7.57 (s, 1H, *H*$_6$-Py), 3.98 (t, 2H, *J* = 7.2 Hz, C*H*$_2$N), 3.55 (t, 2H, *J* = 6.8 Hz, C*H*$_2$O), 2.66-2.61 (m, 1H, C*H*CO), 2.19 (s, 3H, C*H*$_3$-Py), 2.03-2.46, (m, 18H, 9×C*H*$_2$). ^{13}C-NMR (MeOD) δ: 179.41 (*C*=O), 149.19 (*C*$_2$-Py), 147.65 (*C*$_3$-Py), 137.20 (*C*$_4$-Py), 133.81 (*C*$_6$-Py), 103.34 (*C*$_5$-Py), 62.58 (*C*H$_2$O), 51.25 (*C*H$_2$N), 47.97 (*C*HCO), 33.10, 32.74, 29.96, 29.29, 27.79, 23.87, 19.59, 19.46 (9×*C*H$_2$). HPLC analysis: retention time = 11.89 min; peak area 95.50 % (280 nm). HRMS-ESI: m /z calcd for $C_{19}H_{29}BrN_2O_3$ $[M+H]^+$, 413.14343; found 413.14301.

*4.1.8.3. 3-nitro-5-bromo-1-(4-fluorobenzyl)-4-methylpyridin-2(1H)-one (**B7**).*

Purification by flash column chromatography (8:2 hexane-ethyl acetate). Yellow solid (0.024 g, 0.070 mmol, Yield: 39 %). Mp: 152-155 °C. ^{1}H-NMR ($CDCl_3$) δ: 7.55 (s, 1H, *H*$_6$-Py), 7.34, 7.08 (AA'XX' system, 4H, Ar-*H*), 5.11 (s, 2H, PhC*H*$_2$N), 2.28 (s, 3H, C*H*$_3$-Py). ^{13}C-NMR ($CDCl_3$) δ: 163.10 (d, $J_{C\text{-}F}$= 247 Hz, Ar-*C*F), 153.75 (*C*$_2$-Py), 143.46 (*C*$_3$-Py), 138.06 (*C*$_4$-Py), 134.34 (*C*$_6$-Py),130.78 (d, $J_{C\text{-}F}$= 8 Hz, 2×Ar-*C*H), 130.36 (d, $J_{C\text{-}F}$= 3 Hz, Ar-*C*), 116.45 (d, $J_{C\text{-}F}$= 22 Hz, 2×Ar-*C*H), 100.85 (*C*$_5$-Py), 52.25 (Ph*C*H$_2$N), 18.74 (*C*H$_3$-Py). HPLC analysis: retention time = 14.55 min; peak area 95.30 % (280 nm). HRMS-ESI: m /z calcd for $C_{13}H_{10}BrFN_2O_3$ $[M+H]^+$, 340.99316; found 340.99286.

4.2 Biological Assays

4.2.1. Compounds used

All commercial compounds and reagents were purchased from Sigma-Aldrich (Mississauga ON), unless otherwise noted. CP55,940 was purchased from Cayman Chemical (Ann Arbor, MI). All

compounds were initially dissolved in DMSO and diluted in a 10% DMSO solution in PBS. Compounds were added directly to cell culture at the times and concentrations indicated at a final concentration of 0.1% DMSO.

4.2.2. CHO Cells

CHO cells stably transfected with cDNA encoding human cannabinoid CB1Rs or CB2Rs were maintained at 37 °C and 5% CO_2 in Gibco Ham's F-12 nutrient mix supplied by Fisher Scientific UK Ltd. that was supplemented with 2 mM L-glutamine, 10 % FBS, and 0.6 % penicillin−streptomycin, all also supplied by Fisher Scientific UK Ltd. or Canada Ltd., and with the disulfate salt of G418 [(2R,3S,4R,5R,6S)-5-amino-6-{[(1R,2S,3S,4R,6S)-4,6-diamino-3-{[(2R,3R,4R,5R)-3,5-dihydroxy-5-methyl-4-(methylamino)oxan-2-yl]oxy}-2-hydroxycyclohexyl]oxy}-2-[(1R)-1-hydroxyethyl]-oxane-3,4- diol; 600 mg/mL] supplied by Sigma-Aldrich UK. All cells were exposed to 5% CO_2 in their respective media and were passaged twice a week using nonenzymatic cell dissociation solution. For membrane preparation, cells were removed from flasks by scraping, centrifuging, and then freezing as a pellet at −20 °C until required. Before use in a radioligand binding assay, cells were defrosted, diluted in Tris buffer (50 mM Tris-HCl and 50 mM Tris-base). hCB1R and hCB2R CHO-K1 cells were used for data presented in Figures 2-6.

HitHunter® (cAMP) and PathHunter® (βarrestin2) CHO-K1 cells stably-expressing human CB2R (hCB1R) from DiscoveRx® (Eurofins, Fremont, CA) were maintained between passage 5-35 at 37°C, 5% CO_2 in F-12 DMEM (Corning Cellgro, Manassas VA) containing 10% FBS and 1% penicillin-streptomycin with 800 µg/mL geneticin (HitHunter®) or 800 µg/mL geneticin and 300 µg/mL hygromycin B (PathHunter®). HitHunter® and PathHunter® hCB2R CHO-K1 cells were used for data presented in Figure 7.

4.2.3 CB1R and CB2R binding assays

The assays were carried out with [^{3}H]CP55940 and Tris binding buffer (50 mM Tris-HCl, 50 mM Tri-base, 0.1% BSA, pH 7.4), total assay volume 500 μL. Binding was initiated by the addition of transfected hCB1 or hCB2 CHO cell membranes (50 μg protein per well). All assays were performed at 37°C for 60 min before termination by the addition of ice-cold Tris binding buffer, followed by vacuum filtration using a 24-well sampling manifold (Brandel cell harvester; Brandel Inc., Gaithersburg, MD, USA) and Brandel GF/B filters that had been soaked in wash buffer at 4 °C for at least 24 h. Each reaction well was washed six times with a 1.2 mL aliquot of Tris-binding buffer. The filters were oven-dried for 60 min and then placed in 3 mL of scintillation fluid (Ultima Gold XR, PerkinElmer, Seer Green, Buckinghamshire, U.K.). Radioactivity was quantified by liquid scintillation spectrometry. Specific binding was defined as the difference between the binding that occurred in the presence and absence of 1 μM unlabeled CP55,940. The concentration of [^{3}H]CP55,940 used in our displacement assays was 0.7 nM. The compounds used in this investigation were stored as stock solutions of 10 mM in DMSO, the vehicle concentration in all assay wells being 0.1% DMSO. Each point on each graph represents the mean of data obtained from 6 independent experiments. Each experiment was performed in duplicate for each concentration.

4.2.4. Functional activity at CB2R

The GTPγS binding assay was carried out in the presence of [^{35}S]GTPγS (0.1 nM), GDP (30 μM), GTPγS (30 μM), and CHO cell membranes (1 mg/mL) overexpressing hCB1Rs or hCB2Rs. The assay buffer contained 50 mM Tris, 10 mM $MgCl_2$, 100 mM NaCl, 0.2 mM EDTA, and 1 mM DTT (dithiothreitol) at pH 7.4. Incubations were carried out at 30 °C for 90 min in a total volume of 500 mL. The reaction was terminated by the addition of ice-cold wash buffer (50 mM Tris and 1 mg/mL BSA, pH 7.4) followed by rapid filtration under vacuum through Whatman GF/B glass-fiber filters (presoaked in wash buffer), 24-well sampling manifold (Brandel Cell Harvester; Brandel Inc., Gaithersburg, MD, USA), and Brandel GF/B filters that had been soaked in wash buffer at 4°C for at least 24 h. Each reaction well was washed six times with a 1.2 mL aliquot of Tris- binding buffer.

The filters were oven-dried for 60 min and then placed in 3 mL of scintillation fluid (Ultima Gold XR, PerkinElmer, Seer Green, Buckinghamshire, U.K.). Bound radioactivity was determined by liquid scintillation counting. Basal binding of [^{35}S]GTPγS was determined in the presence of 20 mM GDP and absence of cannabinoid. Nonspecific binding was determined in the presence of 10 mM GTPγS. The compounds used in this investigation were stored as stock solutions of 10 mM in DMSO, the vehicle concentration in all assay wells being 0.1% DMSO. Each point on the CP55,940 graph represents the mean of data obtained from 6 independent experiments. Each experiment was performed in duplicate for each concentration.

4.2.5. HitHunter® cAMP assay.

Inhibition of FSK-stimulated cAMP was determined using the DiscoveRx® HitHunter® assay in hCB2R CHO-K1 cells. Cells (20,000 cells/well in low-volume 96 well plates) were incubated overnight in Opti-MEM (Invitrogen) containing 1% FBS at 37°C and 5% CO_2. Following this, Opti-MEM media was removed and replaced with cell assay buffer (DiscoveRx) and cells were co-treated at 37°C with 10 µM FSK and ligands (0.10 nM – 10 µM) for 90 min. cAMP antibody solution and cAMP working detection solutions were then added to cells according to the manufacturer's directions (DiscoveRx®) and cells were incubated for 60 min at room temperature. cAMP solution A was added according to the manufacturer's directions (DiscoveRx®) and cells were incubated for an additional 60 min at room temperature before chemiluminescence was measured on a Cytation 5 plate reader (top read, gain 200, integration time 10,000 ms). n = 6 individual experiments performed in triplicate.

4.2.6. PathHunter® CB1R βarrestin2 assay.

βarrestin2 recruitment was determined using the hCB2R CHO-K1 cell PathHunter® assay (DiscoveRx®). Cells (20,000 cells/well in low-volume 96 well plates) were incubated overnight in Opti-MEM (Invitrogen) containing 1% FBS at 37°C and 5% CO_2. Following this, cells were co-

treated at 37°C with hCB1R ligands (0.10 nM – 10 μM) for 90 min. Detection solution was then added to cells according to the manufacturer's directions (DiscoveRx®) and cells were incubated for 60 min at room temperature. Chemiluminescence was measured on a Cytation 5 plate reader (top read, gain 200, integration time 10,000 ms). n = 3 – 6 individual experiments performed in triplicate.

4.2.7. Statistical Analysis

Data was graphed using GraphPad Prism version 8.02 (GraphPad Software, San Diego, CA). Data are presented as the mean ± the standard error of the mean (S.E.M.) or 95% confidence interval (C.I.) of at least 3 independent experiments conducted in duplicate or triplicate, as indicated. Significance was determined by non-overlapping 95% C.I. or by one-way ANOVA followed by Bonferroni's *post-hoc* test, as indicated. $P < 0.05$ was considered significant. Agonist concentration-response curves were fit to a nonlinear regression (4 parameter) model to determine EC_{50} and E_{Max} in Prism (v. 8.02, GraphPad Software Inc., San Diego, CA).

Acknowledgment

This work was supported by Italian Ministry of Healt – Ricerca Finalizzata 2016 - NET-2016-02363765 and National Interest Research Projects (PRIN 2017, Grant 2017SA5837) to CM, and by a Canadian Institutes of Health Research (CIHR) GlaxoSmithKline partnership grant to RBL (386427). KAM is supported by a National Sciences and Engineering Research Council (NSERC) undergraduate student research award.

Appendix A. Supplementary data

Supplementary data related to this article can be found at

References

[1] I. Katona, T. F. Freund, Multiple functions of endocannabinoid signaling in the brain. Annu. Rev. Neurosci. 35 (2012) 529–558. DOI: 10.1146/annurev-neuro-062111-150420.

[2] S. Banister, K. K. Kumar, V. Kumar, B. K. Kobilka and S. V. Malhotra, Selective modulation of the cannabinoid type 1 (CB1) receptor as an emerging platform for the treatment of neuropathic pain. Med. Chem. Commun. 10 (2019) 647-659. DOI: 10.1039/C8MD00595H.

[3] V. Di Marzo, Targeting the endocannabinoid system: to enhance or reduce? Nat. Rev. Drug Discov. 7 (2008) 438-455. DOI: https://doi.org/10.1038/nrd2553

[4] S. Patel, M. N. Hill, J. F. Cheer, C. T. Wotjak, A. Holmes, The endocannabinoid system as a target for novel anxiolytic drugs. Neuroscience and Biobehavioral Reviews 76 (2017) 56–66. DOI: https://doi.org/10.1016/j.neubiorev.2016.12.033.

[5] L.M. Borgelt, K.L. Franson, A.M. Nussbaum, G.S. Wang. The pharmacologic and clinical effects of medical cannabis. Pharmacotherapy 33 (2013) 195–209. DOI: https://doi.org/10.1002/phar.1187.

[6] A. Oláh, Z. Szekanecz, T. Bíró. Targeting Cannabinoid Signaling in the Immune System: "High"-ly Exciting Questions, Possibilities, and Challenges Front. Immunol. 8 (2017) 1487. DOI: 10.3389/fimmu.2017.01487.

[7] P. Pandey, K. K. Roy, R. J. Doerksen, Negative Allosteric Modulators of Cannabinoid Receptor 2: Protein Modeling, Binding Site Identification and Molecular Dynamics Simulations in the Presence of an Orthosteric Agonist. Journal of Biomolecular Structure and Dynamics. 38 (2020) 32-47. DOI: 10.1080/07391102.2019.1567384.

[8] S. Garai, P.M. Kulkarni, P.C. Schaffer, L.M. Leo, A.L. Brandt, A. Zagzoog, T. Black, X. Lin, D.P. Hurst, D.R. Janero, M.E. Abood, A. Zimmowitch, A. Straiker, R.G. Pertwee, M. Kelly, A.M. Szczesniak, E.M. Denovan-Wright, K. Mackie, A.G. Hohmann, P.H. Reggio, R.B. Laprairie, G.A.Thakur. Application of Fluorine- And Nitrogen-Walk Approaches: Defining the Structural and Functional Diversity of 2-Phenylindole Class of Cannabinoid 1 Receptor Positive Allosteric Modulators. J. Med. Chem. 63(2) (2020) 542-568. doi: 10.1021/acs.jmedchem.9b01142.

[9] F. Gado, S. Meini, S. Bertini, M. Digiacomo, M. Macchia, C. Manera. Allosteric modulators targeting cannabinoid cb1 and cb2 receptors: implications for drug discovery. Future Med. Chem. 11(15) (2019) 2019–2037. DOI: https://doi.org/10.4155/fmc-2019-0005.

[10] F. Gado, L. Di Cesare Mannelli, E. Lucarini, S. Bertini, E. Cappelli, M. Digiacomo, L.A. Stevenson, M. Macchia, T. Tuccinardi, C. Ghelardini, R.G. Pertwee, C. Manera, Identification of the First Synthetic Allosteric Modulator of the CB2 Receptors and Evidence of Its Efficacy for Neuropathic Pain Relief. J. Med. Chem. 62 (2019) 276−287. DOI: https://doi.org/10.1021/acs.jmedchem.8b00368.

[11] R.B. Laprairie, P.M. Kulkarni, J.R. Deschamps, M.E.M. Kelly, D.R. Janero, M.G. Cascio, L.A. Stevenson, R.G. Pertwee, T.P. Kenakin, E.M. Denovan-Wright, G.A. Thakur. Enantiospecific allosteric modulation of cannabinoid 1 receptor. ACS Chem. Neurosci. 8(6) (2017) 1188–1203. DOI: https://doi.org/10.1021/acschemneuro.6b00310

[12] M. Bauer, A. Chicca, M. Tamborrini, D. Eisen, R. Lerner, B. Lutz, O. Poetz, G. Pluschke, J. Gertsch. Identification and Quantification of a New Family of Peptide Endocannabinoids (Pepcans) Showing Negative Allosteric Modulation at CB1 Receptors. J. Biol. Chem. 287(44) (2012) 36944–36967. DOI: https://doi: 10.1074/jbc.M112.382481.

[13] J.G. Horswill, U. Bali, S. Shaaban, J.F. Keily, P. Jeevaratnam, A.J. Babbs, C. Reynet, P. Wong Kai In. PSNCBAM-1, a novel allosteric antagonist at cannabinoid CB1 receptors with hypophagic effects in rats. Br. J. Pharmacol. 152(5) (2007) 805–814. DOI: 10.1038/sj.bjp.0707349

[14] M.R. Price, G.L. Baillie, A. Thomas, L.A. Stevenson, M. Easson, R. Goodwin, A. McLean, L. McIntosh, G. Goodwin, G. Walker, P. Westwood, J. Marrs, F. Thomson, P. Cowley, A. Christopoulos, R.G. Pertwee, R.A. Ross . Allosteric modulation of the cannabinoid CB1 receptor. Mol. Pharmacol. 68(5) (2005) 1484–1495. DOI: https://doi.org/10.1124/mol.105.016162

[15] S. Hryhorowicz, M. Kaczmarek-Rys, A. Andrzejewska, K. Staszak, M. Hryhorowicz, A. Korcz, R. Słomski. Allosteric Modulation of Cannabinoid Receptor 1—Current Challenges and Future Opportunities. Int. J. Mol. Sci. 20 (23) (2019) 5874. DOI:10.3390/ijms20235874.

[16] L.T. May, K. Leach, P.M. Sexton, A. Christopoulos. Allosteric modulation of G protein-coupled receptors. Ann. Rev. Pharm. Toxicol. 47 (2007) 1–51. DOI: https://doi.org/10.1146/annurev.pharmtox.47.120505.105159.

[17] P.R. Gentry, P.M. Sexton, A. Christopoulos. Novel allosteric modulators of G-protein coupled receptors. J. Biol. Chem. 290 (2015) 19478–19488. DOI: 10.1074/jbc.R115.662759.

[18] M. Alaverdashvili, R.B. Laprairie. The future of type 1 cannabinoid receptor allosteric ligands. Drug Metab. Rev. 50 (2018) 50, 14–25. DOI: https://doi.org/10.1080/03602532.2018.1428341

[19] N.T. Burford, M.J. Clark, T.S. Wehrman, S.W. Gerritz, M. Banks, J. O'Connell, J.R. Traynor, A. Alt. Discovery of positive allosteric modulators and silent allosteric modulators of the μ-opioid receptor. Proc. Natl. Acad. Sci. USA. 110 (2013) 10830–10835. DOI: https://doi.org/10.1073/pnas.1300393110

[20] R. Dopart, D. Lu, A.H. Lichtman, D.A. Kendall. Allosteric modulators of cannabinoid receptor 1: Developing compounds for improved specificity. Drug Metab. Rev. 50 (2018) 3–13. DOI: https://doi.org/10.1080/03602532.2018.1428342

[21] T. Nguyen, J.X. Li, B.F. Thomas, J.L. Wiley, T.P. Kenakin, Y. Zhang. Allosteric modulation: An alternate approach targeting the cannabinoid CB1 receptor. Med. Res. Rev. 37 (2017) 441–474. DOI: https://doi.org/10.1002/med.21418

[22] T. Kenakin, L.J. Miller. Seven transmembrane receptors as shapeshifting proteins: the impact of allosteric modulation and functional selectivity on new drug discovery. Pharmacol. Rev. 62 (2010) 265–304. DOI: https://doi.org/10.1124/pr.108.000992

[23] D. Lu, D.E. Potter. Cannabinoids and the cannabinoid receptors: An overview. In Handbook of Cannabis and Related Pathologies Biology, Pharmacology, Diagnosis, and Treatment; Preedy, V.R., Ed.; Academic Press: Cambridge, MA, USA, 2017; pp. 553–563. ISBN 10: 0128007567. ISBN 13: 9780128007563.

[24] R. Greco, C. Demartini, A.M. Zanaboni, D. Piomelli, C. Tassorelli. Endocannabinoid System and Migraine Pain: An Update. Front. Neurosci. 12 (2018) 172. DOI: https://doi.org/10.3389/fnins.2018.00172.

[25] M. Toczek, B. Malinowska. Enhanced endocannabinoid tone as a potential target of pharmacotherapy. Life Sci. 204 (2018) 20–45. DOI: https://doi.org/10.1016/j.lfs.2018.04.054

[26] B.L. Roth, J.J. Irwin, B.K. Shoichet. Discovery of new GPCR ligands to illuminate new biology. Nat. Chem.Biol. 13 (2017) 1143–1151. DOI: https://doi.org/10.1038/nchembio.2490

[27] D. Wootten, A. Christopoulos, P.M. Sexton. Emerging paradigms in GPCR allostery: omplications for drug discovery. Nat. Rev. Drug Discov. 12 (8) (2013) 630–644. DOI: https://doi.org/10.1038/nrd4052

[28] J.S. Smith, R.J. Lefkowitz, S. Rajagopal. Biased signalling: from simple switches to allosteric microprocessors. Nat. Rev. Drug Discov. 17 (4) (2018) 243–260. DOI: https://doi.org/10.1038/nrd.2017.229.

[29] X. Chen, C. Zheng, J. Qian, S. W. Sutton, Z. Wang, J. Lv, C. Liu, N. Zhou. Involvement of β-arrestin-2 and Clathrin in Agonist-Mediated Internalization of the Human Cannabinoid CB2 Receptor. Curr. Mol. Pharmacol. 7(1) (2014) 67-80. DOI: 10.2174/1874467207666140714115824.

[30] R.B. Laprairie, A.M. Bagher, J.L. Rourke, A. Zrein, E.A. Cairns, M.E.M. Kelly, C.J. Sinal, P.M. Kulkarni, G.A. Thakur, E.M. Denovan-Wright. Positive Allosteric Modulation of the Type 1 Cannabinoid Receptor Reduces the Signs and Symptoms of Huntington's Disease in the R6/2 Mouse Model. Neuropharmacology. 151 (2019) 1-12. DOI: 10.1016/j.neuropharm.2019.03.033.

[31] E. Martínez-Pinilla, K. Varani, I. Reyes-Resina, E. Angelats, F. Vincenzi, C. Ferreiro-Vera, J. Oyarzabal, E.I. Canela, J.L. Lanciego, X. Nadal, G. Navarro, P.A. Borea, R. Franco. Binding and signaling studies disclose a potential allosteric site for cannabidiol in cannabinoid CB2 receptors. Front. Pharmacol. 8 (2017) 744. DOI: 10.3389/fphar.2017.00744.

[32] Z. Feng, M. H. Alqarni, P. Yang, Q. Tong, A. Chowdhury, L. Wang, X.Q. Xie. Modeling, Molecular Dynamics Simulation, and Mutation Validation for Structure of Cannabinoid Receptor 2

Based on Known Crystal Structures of GPCRs. J. Chem. Inf. Model. 54(9) (2014) 2483-2499. DOI: 10.1021/ci5002718.